A4WP-QI COMBO SYSTEM FOR CONTINIOUS WIRELESS CHARGING RANGE COVERAGE WITH RESONANCE FILTERING

A Thesis

by

Üstün Sağlam

Submitted to the

Graduate School of Sciences and Engineering
In Partial Fulfillment of the Requirements for
the Degree of

Master of Science

in the
Department of Electrical and Electronics Engineering

Özyeğin University
January 2019

A4WP-QI COMBO SYSTEM FOR CONTINIOUS WIRELESS CHARGING RANGE COVERAGE WITH RESONANCE FILTERING

Approved by:

Asst. Prof. Ahmet Tekin, Advisor,
Department of Electrical and Electronics Engineering
Özyeğin University

Asst. Prof. Göktürk Poyrazoğlu,
Department of Electrical and Electronics Engineering
Özyeğin University

Asst. Prof. Özgür Tamer,
Department of Electrical and Electronics Engineering
Dokuz Eylül University

Date Approved: 2 January 2019

To my family…

ABSTRACT

Distribution of wireless power charging field uniformly on a large area pad is critical for receivers, especially for wearable devices because of their small form factor receiver coil. Since the receiver coil size is quite limited in these types of technologies; the device is very sensitive to the amount of field it could retain and it needs special placement or snapping to fix it at an optimum location for reliable charging. In order to overcome this problem, a dual-mode multi-coil power transceiver system is proposed; utilizing resonance filtering to increase the amount of total power delivered with rather uniform spacial distribution. Two concentric coils; one driven by 6,78-MHz high frequency driver (A4WP) and the other with a 200-KHz low frequency driver (Qi) with resonant blocker could transfer 30mW to 50mW standards compliant flat power to a 13-mm radius 30-turns wearable receiver coil everywhere across an 8cm radius charging pad area without any alignment requirement or snapping.

ÖZET

Büyük ped üzerindeki kablosuz şarj alanının eşit dağılımı alıcılar için özellikle de küçük formlu alıcı bobinlerinden dolayı giyilebilir cihazlar için kritik öneme sahiptir. Bu tür teknolojilerde alıcı bobin büyüklüğü oldukça sınırlı olduğundan; cihaz yakalayabileceği alan miktarına çok duyarlıdır ve güvenilir şarj için cihazın özel bir yerleşime veya en uygun yerde sabitlenmesine gerek vardır. Bu problemin üstesinden gelmek için, daha eşit uzaysal dağılım ile aktarılan toplam güç miktarını artırmak için rezonans filtrelemeden yararlanarak çift modlu çok bobinli güç alıcı-verici sistemi önerilmiştir. Biri 6,78MHz'de yüksek frekansla sürülen ve diğeri 200kHz'lik düşük frekansla sürülen iç içe iki bobin, rezonant engelleyici filtre ile 13mm yarıçaplı 30 tur oranı olan giyilebilir cihazın alıcı bobinine hizalama ve sabitleme gerektirmeden 8cm yarıçaplı şarj pedi alanının her yerinde 30mW'tan 50mW'a kadar standartlara uyumlu sabit güç aktarabilir.

ACKNOWLEDGMENTS

During my thesis study, Asst. Prof. Ahmet Tekin gave to me his support. He showed me the target and always motivated to me to get it. He guided to me as a real advisor.

I would also like to thank my colleagues Cengiz Tarhan and Mert Serdar Bilgin in Vestel Electronics. They were helpful and considerate.

Another thanks to my family. They stand always behind me.

TABLE OF CONTENTS

LIST OF TABLES

,

LIST OF FIGURES

CHAPTER I

INTRODUCTION

It is needed to provide electrical energy for all electronic devices to work. Some devices are connected to a grid and some of them include battery. In recent years, the usage of wireless power transfer systems is increasing in all areas of our life due to ease of use. Furthermore, they are safer than the traditional systems and they also eliminate cable clutter [1]. Wireless systems will become even more important with the increase of the usage of electronic devices and the increase of complications in connecting these devices to each other. Some applications have already been using this technology such as consumer electronics, automotive, biomedical.

1.1 Introduction to Wireless Power Transfer

Traditional power transfer systems need wires to contact transmitter side and receiver side. Transmitter side supplies power and receiver side consumes power. In wireless power transfer systems, there isn't any electrical contact between transmitter and receiver, and it works in the principle of generating electromagnetic fields and transferring the energy through air gap. There are different methods of wireless power transfer technology related to transferred power level and the distance between transmitter and receiver. The distance factor divides the technology into two parts as near field and far field. In near field applications, electrodynamic induction coupling via magnetic fields is mostly preferred. This method is also divided into two different ways in itself. One of them is

inductive coupling method and the other one is magnetic resonance coupling method. Microwave and laser are the kinds of radiative transfer for far fields. They can carry an information to longer distances. Low level power transfer is achievable in long range transfer methods due to lossy ambient [2].

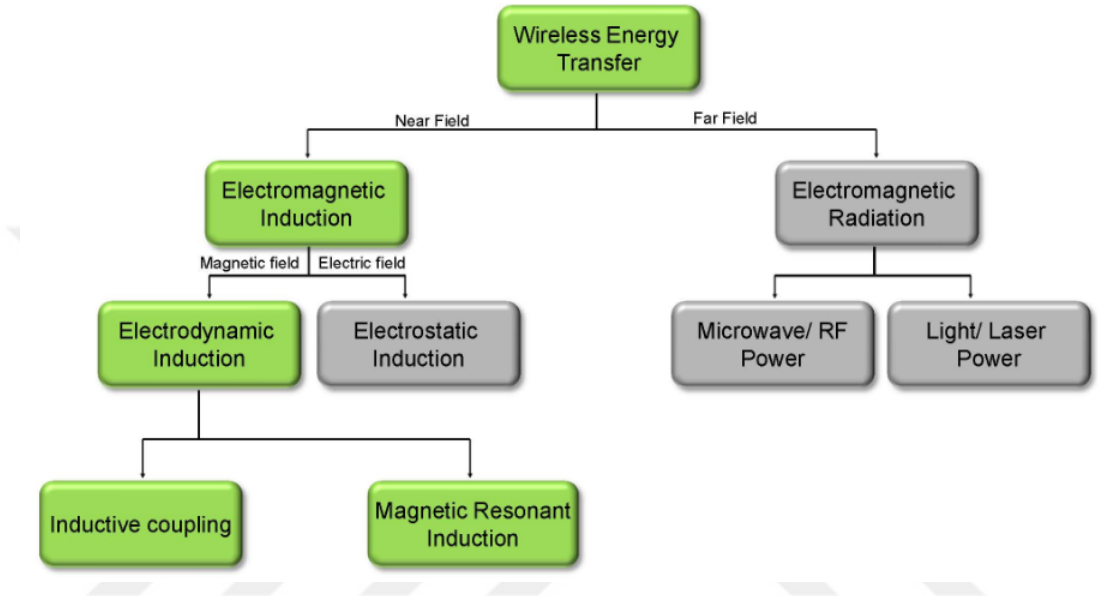

Figure 1.1: A diagram of wireless energy transfer types [3].

Transformers transfer the energy from primary windings to secondary windings through a core. An alternating current on primary winding creates magnetic fields based on Ampere's law and the magnetic fields induce voltage on secondary winding based on Faraday's law [4]. The magnetic material core has higher permeability than air in order to create a low impedance path for generated magnetic fields. If the magnetic fields pass through the air-core instead of the magnetic material-core, this method would become inductively coupled wireless power transfer. An alignment of transmitter and receiver coils is critical with related to mutual inductance. Better coupling factor means less distance between transmitter and receiver [5]. The distance between transmitter and receiver is just a few millimeters in inductively coupling method [6].

Resonant coupling method allows higher distance power transfer than inductively coupling method. Transmitter circuit and receiver circuit must tune at the same resonance frequency. Tuning the circuits is the challenge of resonant coupling method. Due to the narrow bandwidth of the resonance frequency, a little bit frequency shift causes major efficiency loss [6]. This system has loosely coupled coils. System efficiency is better in tightly coupled coils than loosely coupled coils [3].

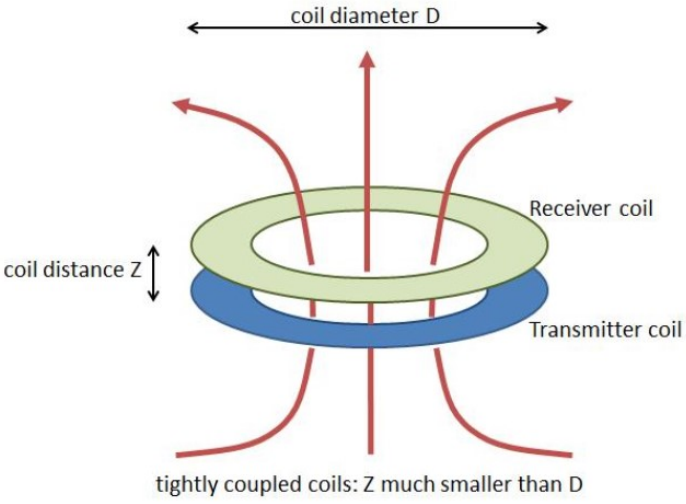

Figure 1.2: Tightly coupled coils [3].

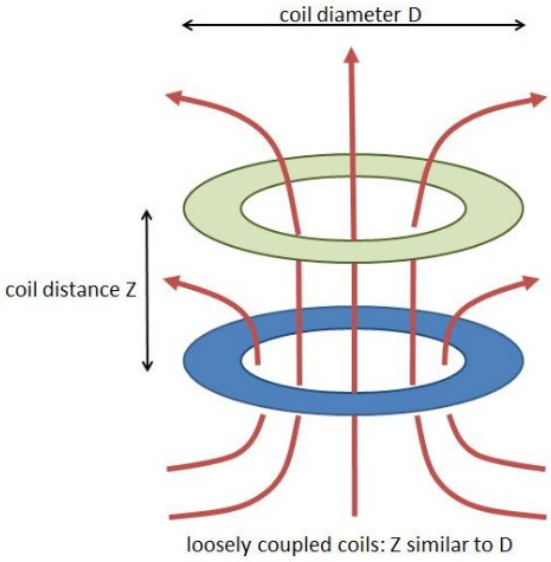

Figure 1.3: Loosely coupled coils [3].

Generally, input power is supplied to the wireless charging system by the AC grid in both of inductive coupling and resonant coupling methods. Firstly, AC must be rectified to DC. Then, a driver circuit is used to create current changes that would generate magnetic fields from the coil. Frequency of the driver is adjusted according to the standard which would be compliant. Induced voltage on the receiver coil is rectified and filtered to charge the battery. In accordance with the load condition, communication as a feedback is provided between the receiver controller and the transmitter controller [3][7].

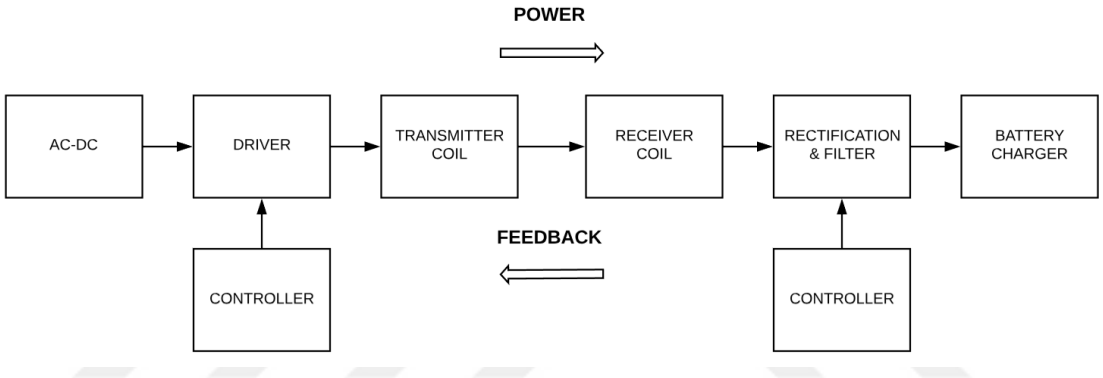

Figure 1.4: General block diagram of wireless power transfer system

1.2 Wireless Power Transfer Standards

There are some wireless power transfer standards that have been developed to make transmitter and receiver compliant with each other. Standards ensure general usage worldwide. There are three different standards: Qi, A4WP and PMA. Qi standard belongs to Wireless Power Consortium (WPC), Alliance for Wireless Power (A4WP) and Power Matters Alliance (PMA). A4WP and PMA are formed as AirFuel Alliance [8]. These standards have some advantages and disadvantages with respect to each other.

1.2.1 Qi Standard

Wireless Power Consortium is established in 2008. Qi Standard's method was an inductive power transfer at first. It has wide frequency range from 87kHz to 205kHz [9]. The systems that compliant with Qi standard have high efficiency by inductive coupling method [10]. Because of the necessity of using inductive coupling method, coupling coefficient must be close to 1 which is the maximum value of the coefficient as much as possible [11]. It means that the distance between transmitter and receiver has to be just a few millimeters [10]. Transmitter can supply only one receiver at a time and the alignment of receiver over the transmitter is critical for coupling to better efficiency [12]. This standard also has better EMI performance [3].

- **V1.0 – V1.1**
  - ✓ Inductive power transfer method
  - ✓ Communication is performed by load modulation in-band
  - ✓ Distance between TX and RX is about a few millimeters
  - ✓ Power transfer is limited to 5W
  - ✓ Single transmitter can charge only one receiver at the same time
- **V1.2**
  - ✓ Maximum power is increased to 15W
  - ✓ Added resonant power transfer compatibility
  - ✓ Ability to charge multiple receivers
  - ✓ Improved power transfer distance
  - ✓ Free positioning

1.2.2 A4WP Standard

A4WP Standard allows resonant induction method and operate at 6,78MHz ISM band. Tolerances of this center frequency are just ±15kHz which is much narrower than Qi Standard's allowed frequency limits [13]. Tight frequency limits for A4WP make the frequency control difficult because of environment dependent factors in the system [13]. It can be designed small form factor coils with relatively high quality factor [11], and the ripple performance of the output voltage of receiver is better due to high operating frequency. Huge magnetic field is another benefit of high frequency. Despite these advantages of high frequency, parasitic effects occur and efficiency decreases as switching losses increase [14].

- ✓ Large power transfer distance (about 50mm)
- ✓ Free positioning
- ✓ One transmitter can charge more than one receiver at the same time
- ✓ Communication is performed via Bluetooth (2,4GHz)

1.2.3 PMA Standard

Inductive power transfer method is used in PMA Standard. Operating frequency range is from 277kHz to 357kHz [8]. This standard's characteristics are mostly similar to Qi.

- ✓ Communication is performed in-band
- ✓ Distance between TX and RX is about a few millimeters
- ✓ Power transfer is limited to 5W

Table 1.1: A comparison of WPT standards

	Qi (V1.2)	PMA	A4WP
Technology	Inductive coupling, Resonant inductive	Inductive coupling	Resonant inductive
Efficiency	Higher	Higher	Lower
Power transfer distance	5mm (inductive), 45mm (resonant)	5mm	50mm
Power level	Low power - 15W High power - 200W Kitchen - 2000W	15W	50W
Frequency	87-205kHz	277-357kHz	6.78MHz
Free positioning	Yes	No	Yes
Multiple receivers	Multiple	Single	Multiple
Communication	In-band	In-band	Bluetooth
Cost	Low	Low	High
Available products	High	Medium	Low
Switching losses	Low	Low	High
Output voltage ripple	Higher	Higher	Lower

1.3 Key Factors of Wireless Power Transfer

In order to increase the efficiency of a wireless charging system, magnetic shielding method is helpful and generally, used in systems. They can be used under the transmitter coil, above the receiver coil or the both together. Ferrite sheet provides low impedance to magnetic field which passes through it [15]. Thus, loss in magnetic field decreases and coupling between transmitter and receiver coils increases, hence the overall transfer efficiency as elaborated in some studies [16][17]. With the presence of ferrite sheet under the transmitter coil, the inductance of the transmitter coil also increases. Magnetic shielding enhances the coupling and as a result of it, reliable power transfer distance between transmitter and receiver could increase. Effectiveness of the shielding depends on permeability and thickness of the magnetic sheet.

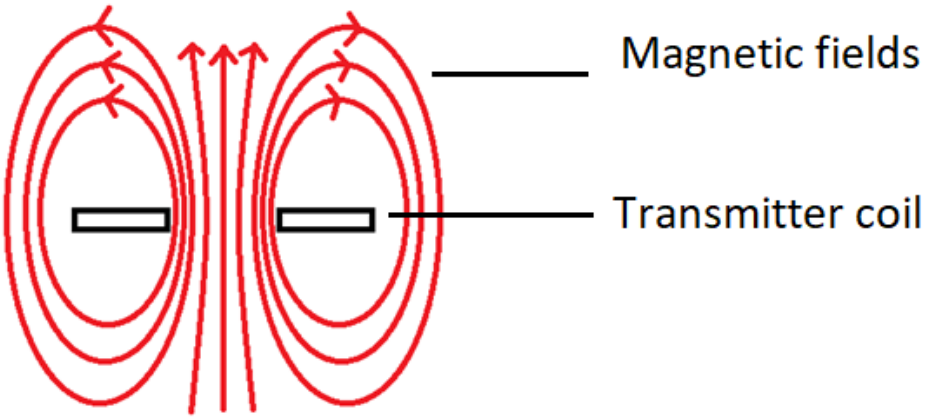

Figure 1.5: Generated magnetic fields by transmitter coil

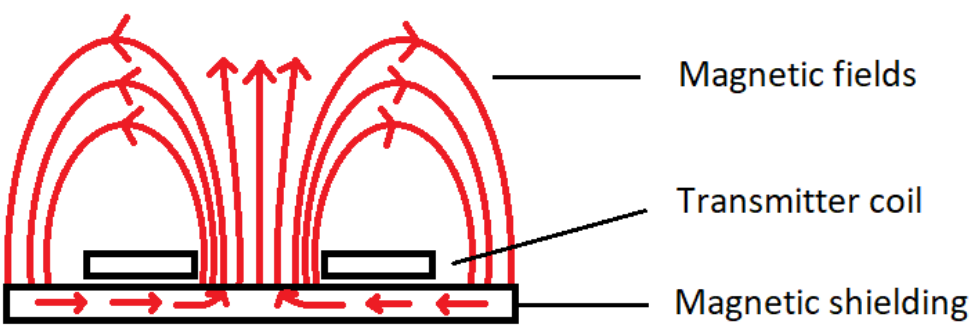

Figure 1.6: Generated magnetic fields by transmitter coil with magnetic shielding

Alignment is critical factor for inductive coupling method. If the alignment between transmitter and receiver is not well, coupling coefficient would be low [3]. Efficiency is proportional to the coupling coefficient [3]. Generated magnetic fields by charging pad affects transferred power level directly. If the magnetic field is strong enough, receiver could be induced highly efficient. But if it is weak, receiver couldn't supply the load. When the transmitter coil's size and receiver coil's size are not equal like wearable device on a larger charging pad, loosely coupled coils structure is occurred [3]. By this way, uniform power supply couldn't realize. Multiple transmitters could be used to achieve misalignment problem on tightly coupled coils. Thus, positioning freedom

could be provided horizontally [3]. Additionally, multiple transmitters bring the capability of charging multiple receivers at the same time [3]. Multiple transmitter coils are placed in overlapped structure generally.

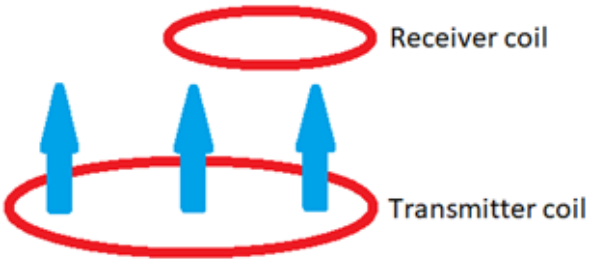

Figure 1.7: Loosely coupled coils due to non-equal sizes

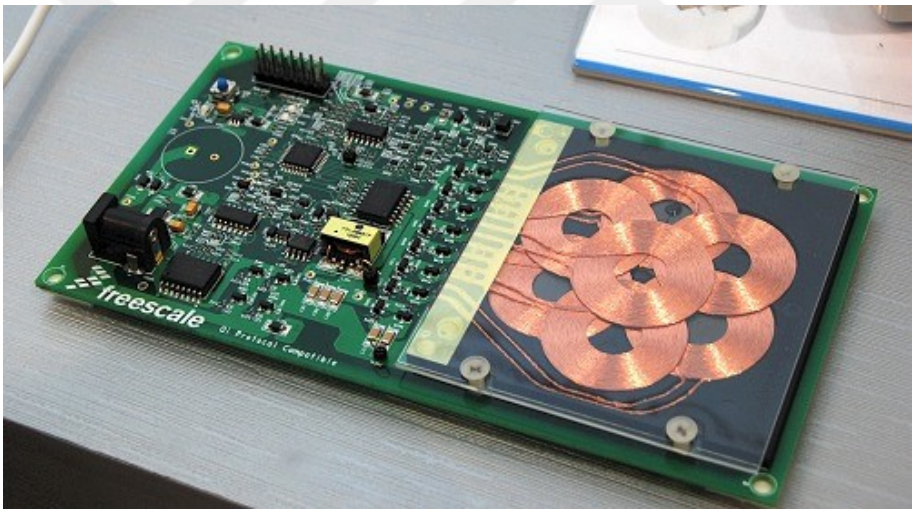

Figure 1.8: Multiple transmitter coils [3].

Increasing distance in Z-direction makes the system loosely coupled. Free positioning in three dimensions is possible only by resonant coupling method.

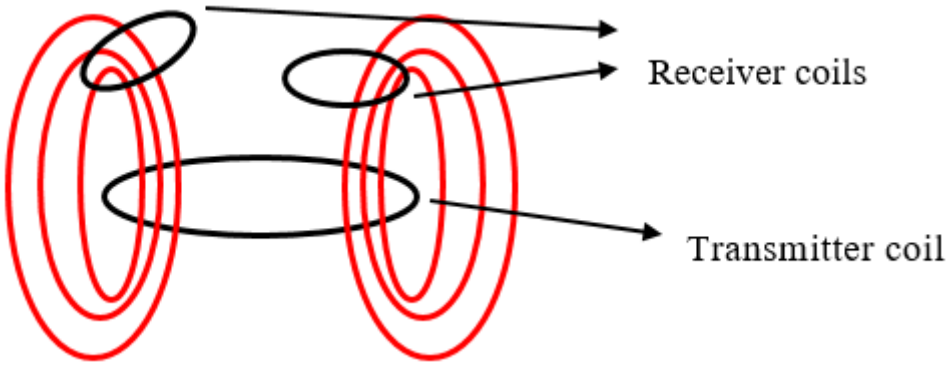

Figure 1.9: Free positioning in resonant coupling

Designing both Qi and A4WP compliant systems is an active research topic to take advantage of the benefits of the both. Each power receiver device, which belongs to a particular wireless charging standard, needs a transmitter that should resonate along with the same standard specifications. There is a significant amount of research effort underway to combine different standards with full compatibility on receiver side or even on transmitter side. In [18], both 200kHz and 6,78MHz supported transmitters and receivers are studied. This system is developed to negotiate negative interactions between the 200kHz and the 6,78MHz pieces. This particular system works in dual band. 200kHz and 6,78MHz supported transmitters transfer the energy to 200kHz and 6,78MHz supported receivers, respectively. In [19]-[21], tradeoffs with respect to different wireless power standards were studied. In [14], low and high frequency effects were studied based on receiver side.

Wireless charging of wearable devices is a particularly hard task to implement because of the small form factor receiver coils. Suggested wireless charging systems require large receiver coils to collect energy from the generated magnetic field. However, the size is quite limited in wearable devices. Hence, coupling would be weak and efficiency would be low. Research done in the field recently shows that the size, cost and efficiency must all be considered carefully in wearable devices [13][22][23]. It is

particularly hard to drive the small form factor receiver coil since the transmitted power level changes wildly according to the placement of receiver (RX) coil on a large charging pad. Large transmitter (TX) coil doesn't generate equal magnetic field strength across all the points along the pad. Hence, the coupling factor, k, and the power delivered to the load change depending on the location. Uniformity of generated magnetic field, hence, becomes a quite key design consideration. The other important design criterion for small form factor receivers is the total amount of spacially uniform power that could be delivered to a receiver.

1.4 Scope of Thesis

The aim of the thesis is research and design of a Qi and A4WP compliant combo power transfer system for small form factor wearable device applications. The combo system has not only helped the total amount of power that could be transferred, but also assured spacial charging uniformity across the wide charging pad which resulted in more comfort in user experience. Design tradeoffs in relation to concurrent multi-driver co-centric coil design as well as performance enhancement due to the proposed resonant filtering technique were all discussed in detail along with the measurements from the actual design prototypes.

CHAPTER II

THEORY

2.1 Analysis of Wireless Power Transfer Systems

The concept of inductive coupling is based on two laws. Ampere's Law means that the flowing current on a wire generates magnetic fields. Faraday Law means that changing magnetic fields induce an electromotive force on coil. Electromotive force is the potential difference on coil. These two laws explain the magnetic theory of power transfer via magnetic fields.

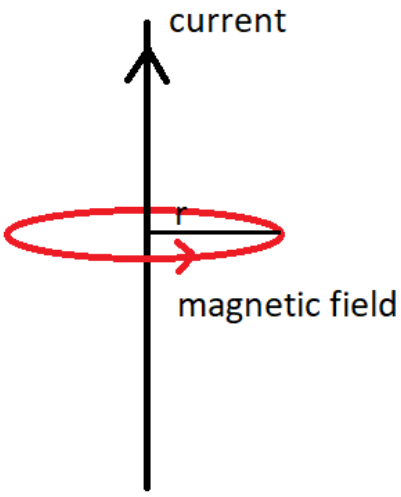

Figure 2.1: Ampere's Law

$$\oint \vec{\boldsymbol{H}}.d\vec{\boldsymbol{l}} = I \qquad (1)$$

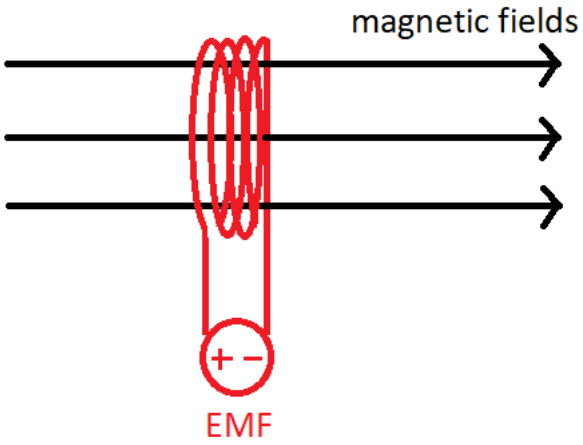

Figure 2.2: Faraday's Law

$$V = -N\frac{d\Phi}{dt} \tag{2}$$

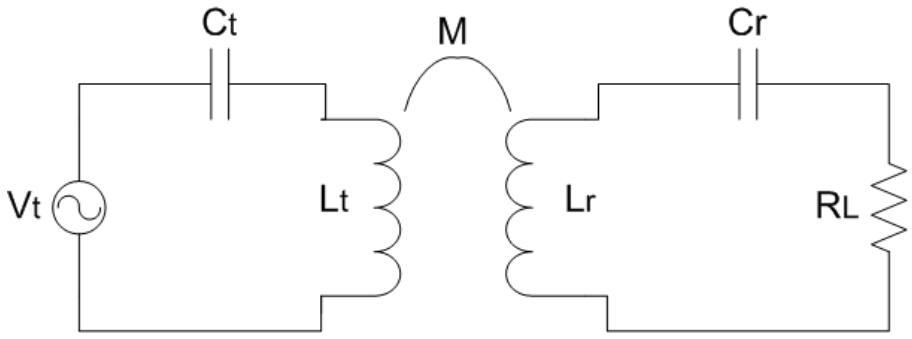

Figure 2.3: An equivalent WPT circuit

A general used wireless power transfer circuit is shown in Figure 2.3. There are alternating voltage source of transmitter (V_t), a transmitter coil (L_t) and a decoupling capacitor for resonance condition (C_t) in series with the coil. A receiver coil (L_r) that is coupled to the transmitter coil, a capacitor (C_r) in series to the receiver coil and a load

exist on the receiver side. Coupling condition of L_t and L_r creates mutual inductance (M). Rating of mutual inductance to the self-inductance of transmitter and receiver coils is defined as coupling coefficient (k). As coupling would be better, coupling coefficient approaches to 1 which is its maximum value. If the distance between the transmitter and the receiver increases, the coupling decreases. Thus, the efficiency would be also low.

$$k = \frac{M}{\sqrt{L_t\, L_r}} \tag{3}$$

In the inductively coupled system, coupling coefficient values are between 0,2 and 0,7 approximately. It depends on tightly coupled coils. Since the tight coupling, leakage inductance value is less than magnetizing inductance. Voltage gain between receiver and transmitter is proportional to the coupling coefficient and ratio of inductances shown in (4). Two parameters determine the capability of power transfer. These parameters are open-circuit voltage (V_{oc}) and short-circuit current (I_{sc}). In I_{sc} formula, coil losses (R_r) is assumed negligible.

$$\frac{V_r}{V_t} \rightarrow k\sqrt{\frac{L_r}{L_t}} \tag{4}$$

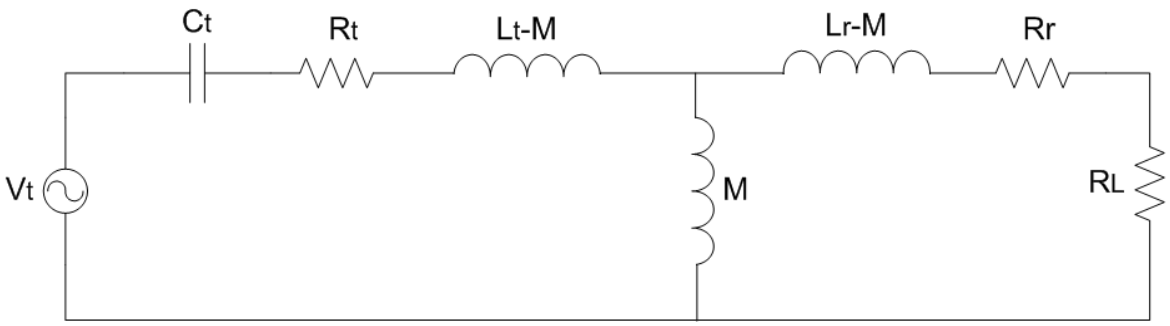

Figure 2.4: T-equivalent circuit of inductive coupled WPT

$$V_{oc} = j\omega M I_t \tag{5}$$

$$I_{sc} = I_t \frac{M}{L_r} \tag{6}$$

$$S = V_{oc} I_{sc} = \omega I_t^2 \frac{M^2}{L_r} \tag{7}$$

$$P_{o,max} = \frac{1}{2} V_{oc} I_{sc} \tag{8}$$

$P_{o,max}$ is the maximum delivered power to the load. The delivered power to the load could be increased with the resonance condition. To get the resonance condition on the receiver side, the capacitor must be added to the receiver circuit shown in Figure 2.6. Series capacitors reduce the loss which is caused by leakage inductance. The delivered power to the load could increase by Q times. Q is the quality factor of the receiver. Although higher Q means higher power transfer, it reduces the bandwidth. Bandwidth is the frequency range where meaningful power transfer could be obtained corresponding to the operational frequency.

$$Q = \sqrt{\frac{L_r}{C_r}} \frac{1}{R_L} = \frac{\omega L_r}{R_L} \tag{9}$$

$$BW = \frac{\omega}{Q} \tag{10}$$

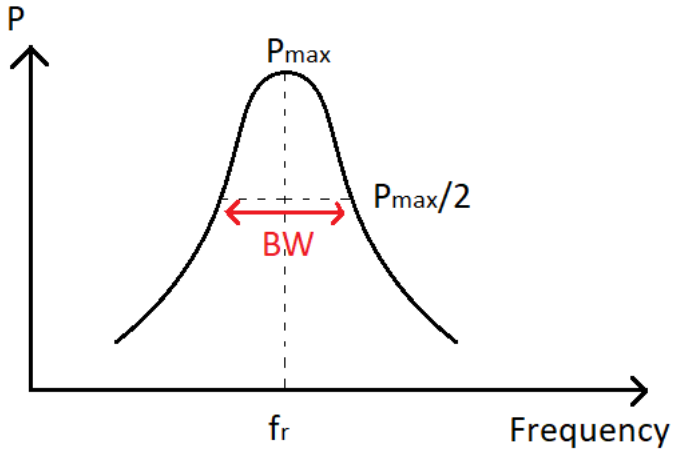

Figure 2.5: A graph of bandwidth

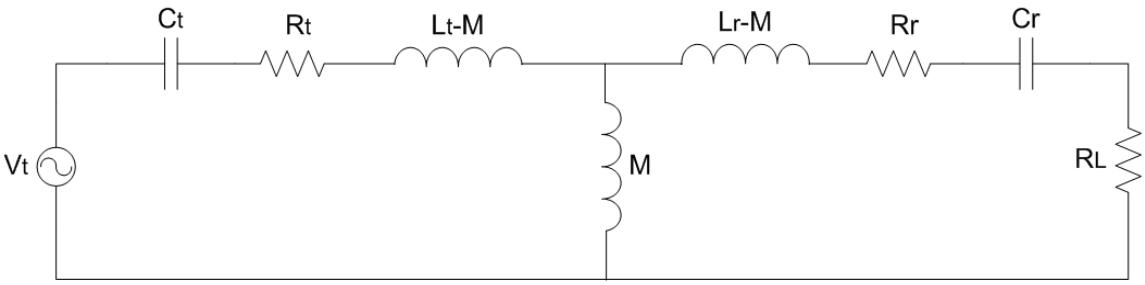

Figure 2.6: T-equivalent circuit of resonant WPT

$$V_t = I_t\left(R_t + j\omega(L_t) + \frac{1}{j\omega C_t}\right) - I_r(j\omega M) \tag{11}$$

$$I_t(j\omega M) = I_r\left(R_r + j\omega(L_r) + \frac{1}{j\omega C_r} + R_L\right) \tag{12}$$

$$Z_{in} = \frac{V_t}{I_t} = R_t + j\left(\omega(L_t - M) - \frac{1}{\omega C_t}\right) + Z_p \tag{13}$$

$$Z_p = \frac{Z_s j\omega M}{Z_s + j\omega M} \tag{14}$$

$$Z_s = R_r + R_L + j\left(\omega(L_r - M) - \frac{1}{\omega C_r}\right) \tag{15}$$

The resonance frequency is described as formula (16). In resonance condition, the transmitter and the receiver have to tune at the same resonance frequency. Thus, impedance seen from the input is delivered in (19), by using the following equation.

$$\omega_0 = \frac{1}{\sqrt{LC}} \tag{16}$$

$$\omega_0 = \omega_t = \omega_r \tag{17}$$

$$\frac{1}{\sqrt{L_t C_t}} = \frac{1}{\sqrt{L_r C_r}} \tag{18}$$

$$R_{in} = R_t + \frac{k^2 L_t}{C_r(R_r + R_L)} = R_t + \frac{\omega^2 M^2}{R_r + R_L} \tag{19}$$

The efficiency of the system is the ratio of the output power to the input power. The difference between output and input powers occur due to the losses on the circuit. The efficiency (η) of the system is described as:

$$\eta = \frac{P_{out}}{P_{in}} = \frac{I_r^2 R_L}{I_t^2 Z_{in}} \tag{20}$$

In the resonance condition, high sinusoidal voltage occurs. The peak voltage seen on the capacitor increases due to higher Q.

$$V_{c,peak} = Q \frac{2V_t}{\pi} \tag{21}$$

In order to increase the delivered power to the receiver by transmitter, the transmitter must supply high voltage and high current. There are limits on the system that are caused by driver circuit or coils. High voltage or high current may affect heating, cost or size. But, in order to get efficient power, transmitter must supply high current and high voltage within its limits. In accordance with the coupling cases, efficiency and characteristic of the system changes.

- Over-critical coupling: $k.Q > 1$
- Critical coupling: $k.Q = 1$
- Under-critical coupling: $k.Q < 1$

In over-critical coupling, driver circuit limits the transmitted power. Unstable resonance frequencies occurred in over-critical coupling condition. Critical coupling condition is the ideal one. Under-critical coupling is the least efficient condition. Under-critical coupling can be caused by low k or high R_L.

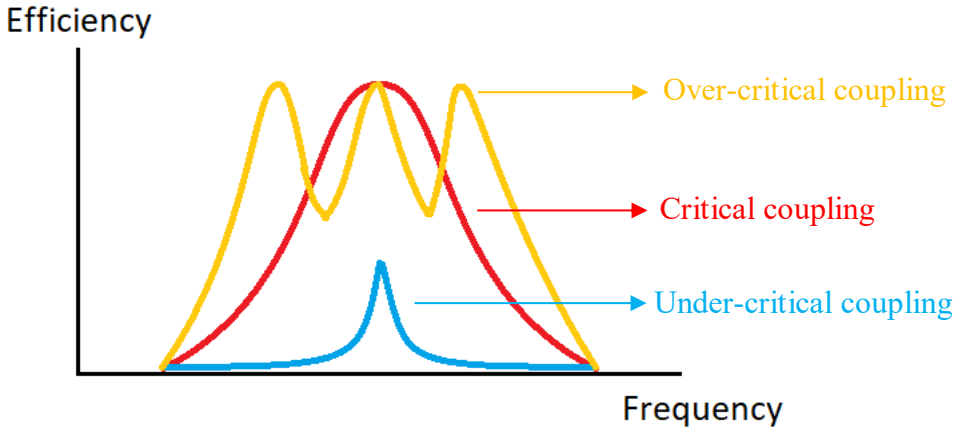

Figure 2.7: Efficiency vs. Frequency according to the coupling cases

2.2 Types of Resonant Circuits

In resonant topologies, inductor and capacitor are used to tune at the resonance frequency. Tuning is provided by series, parallel and series-parallel compensation circuits. These circuits should be chosen according to the system requirements in transmitter and receiver side. Series compensation circuit acts like a short circuit at resonance frequency due to impedances of capacitor and inductor. Otherwise, parallel compensation acts like an open circuit. Thus, series compensation circuit is like a current source and parallel compensation circuit is like a voltage source. It depends on the requirements of the system.

Parasitic effects of capacitor may affect frequency much more in series compensation circuits. Wireless power transfer systems have high leakage inductance due to distance. If the distance increases, leakage inductance increases proportionally. Capacitor could eliminate the leakage inductance in series resonant circuits. Thus, higher power transfer would be available. In parallel resonant, capacitor could eliminate magnetizing inductance, so higher efficiency could be obtained. Resonant circuit could

increase the supply voltage of the transmitter coil from driver voltage in series compensation which ensures high transmitter coil inductance. On the other hand, parallel compensation increases driver current. Series-parallel topology (LCC topology) could provide eliminating leakage effect and tuning magnetizing inductance. It provides better impedance response.

If the secondary side is in series structure, no reflected reactance is seen from primary side. Otherwise, when secondary side is in parallel compensation structure, reflected reactance of secondary side is seen from primary side. Reflected reactance would be frequency dependent. SP topology, series in transmitter and parallel in receiver, supplies stable current and PS topology, parallel in transmitter and series in receiver, supplies stable voltage. On the other hand, LCC topology has lower efficiency than LLC topology, but better misalignment performance.

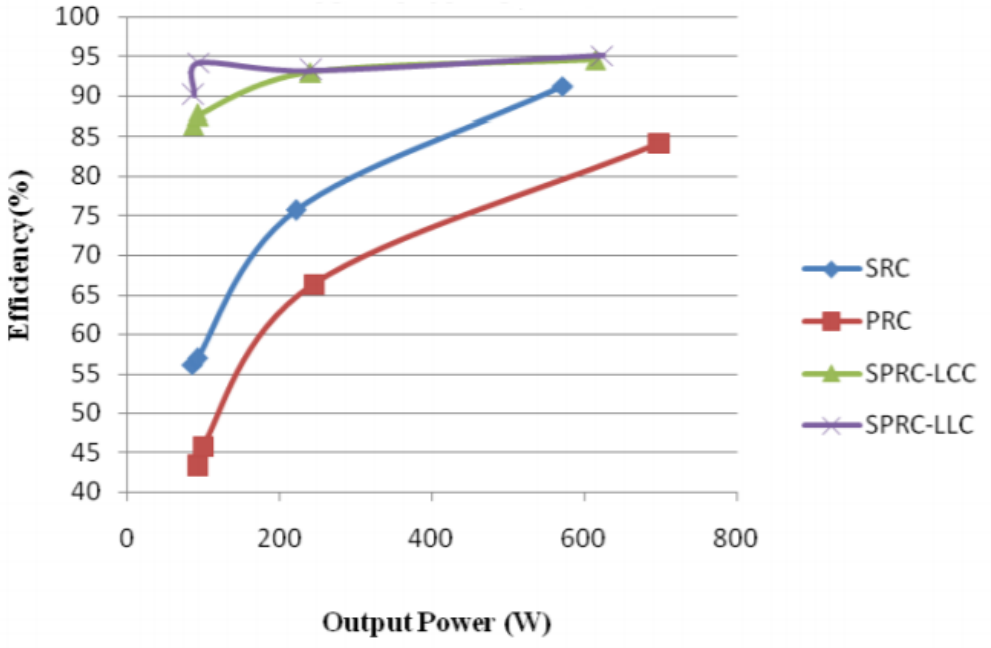

Figure 2.8: Comparison of efficiencies of resonant converter topologies

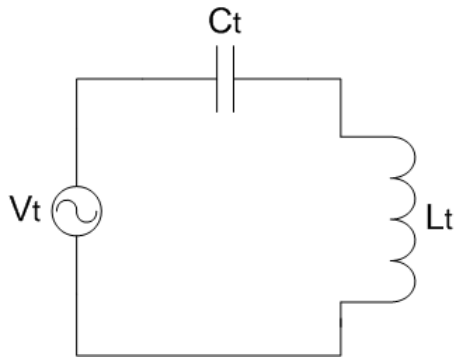

a)

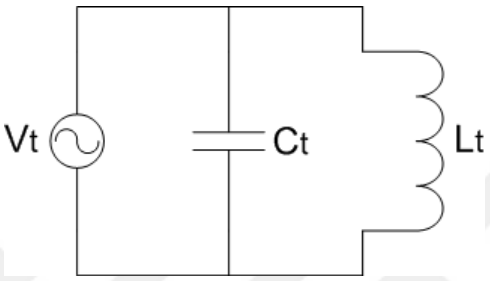

b)

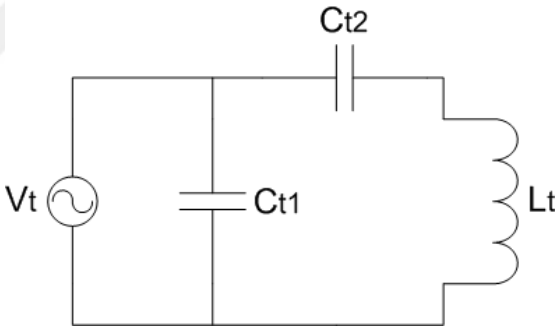

c)

Figure 2.9: Resonance compensation types in transmitter a) series b) parallel c) series-parallel

$$C_{t1} = \frac{1}{\omega^2 M} \tag{22}$$

$$C_{t2} = \frac{1}{\omega^2(L_t - M)} \tag{23}$$

Series compensation in receiver side generates the output voltage on the load, V_{oc}, and the current is defined to the load. Parallel compensation is just the opposite of series compensation and current would be I_{sc} because of the circuit acts as a current source. Receiver side series-parallel compensation circuit is used in Qi standard. C_{r1} resonates with L_r and C_{r2} resonates at 1MHz with L_r due to requirement of Qi specification.

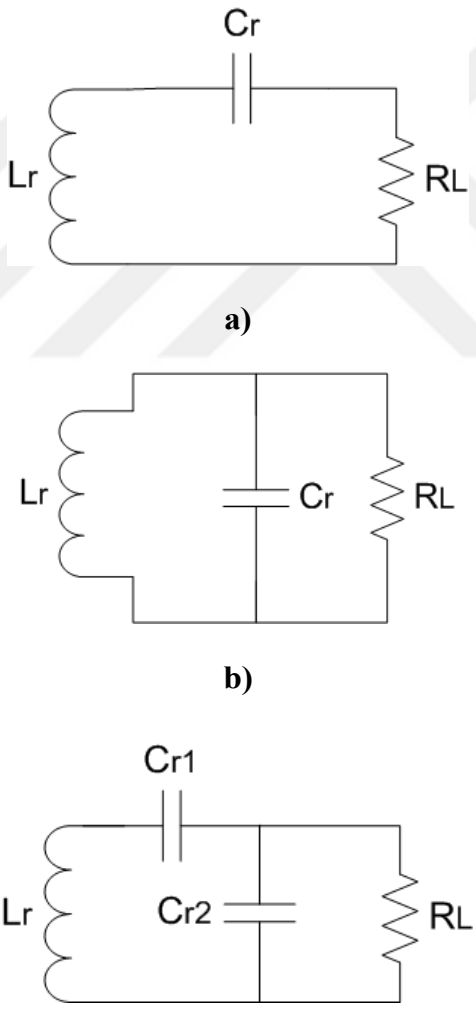

Figure 2.10: Resonance compensation types in receiver a) series b) parallel c) series-parallel

Reflected resistance of the load for series compensation on receiver side:

$$R_{L,r} = \frac{\omega^2 M^2}{R_L} \tag{24}$$

Reflected resistance of the load for parallel compensation on receiver side:

$$R_{L,r} = \frac{M^2 R_L}{{L_r}^2} \tag{25}$$

In parallel compensation circuit, quality factor (Q) would be:

$$Q = \frac{R_L}{\omega L_r} \tag{26}$$

$$C_{r2} = \frac{1}{(10^6.2\pi)^2 \left(L_r - \frac{1}{C_{r1}}\right)} \tag{27}$$

2.3 Comparison of Driver Circuits

In order to drive the transmitter coil, an amplifier circuit is required. There are a few inverter topologies that are used generally in wireless power transfer applications. Driver circuits are used together with resonant tanks to create sinusoidal waveforms. Class E and Class D inverters are most common topologies.

Class E inverter allows high frequency operations and transfers high power levels up to kW ranges. Due to zero-voltage switching, switching losses are less. Thus, efficiency could be high. Another benefit of Class E is the low cost due to less

components. High voltage peaks on the switching device is the disadvantage of the Class E topology. Class E circuit parameters must be tuned.

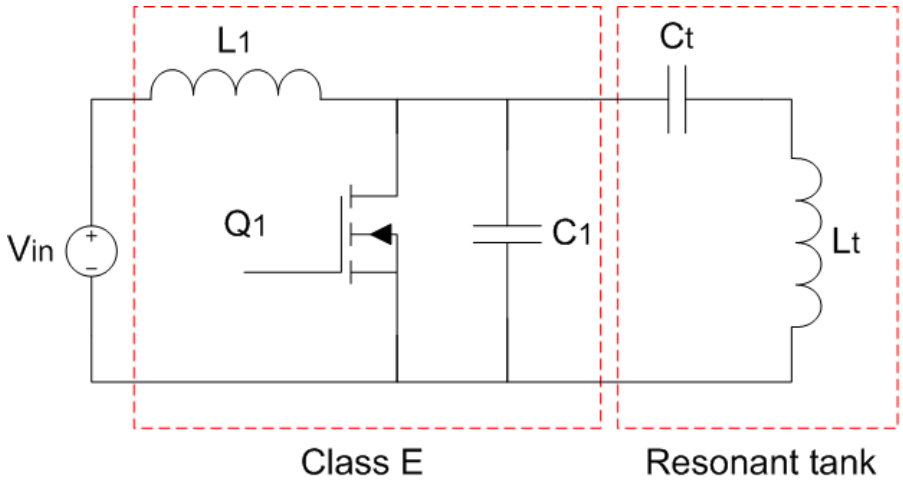

Figure 2.11: Class E driver circuit

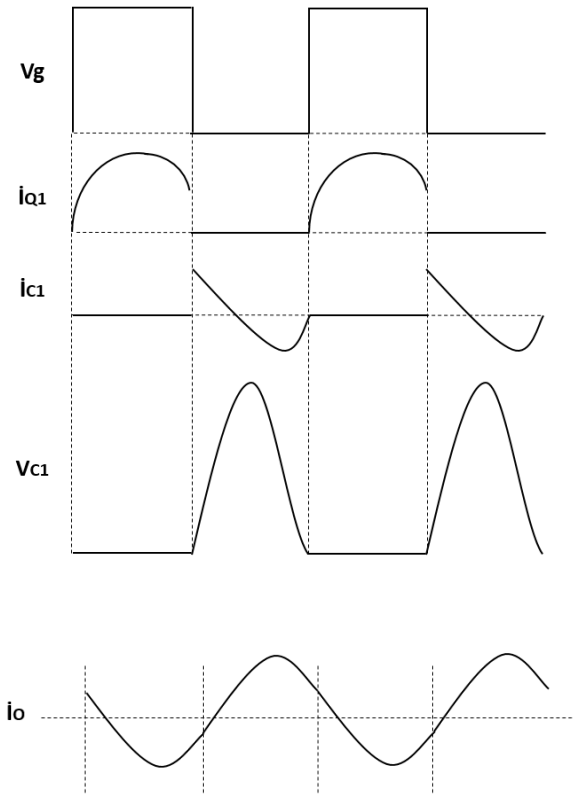

Figure 2.12: Waveforms of Class E

Class D topology is a better choice when the input supply voltage is low. Class D topology has three different types. One of them is half bridge with two switches, the other one is full bridge (H-bridge) and at last Class DE type which is derived from Class D by adding capacitors parallel to the switches. Voltage stress on switches is lower in compare to Class E. Power transfer capability of full bridge is higher than the half bridge. Voltage stress on Class DE is the lowest one because of parallel capacitors. These capacitors also provide lower switching loss.

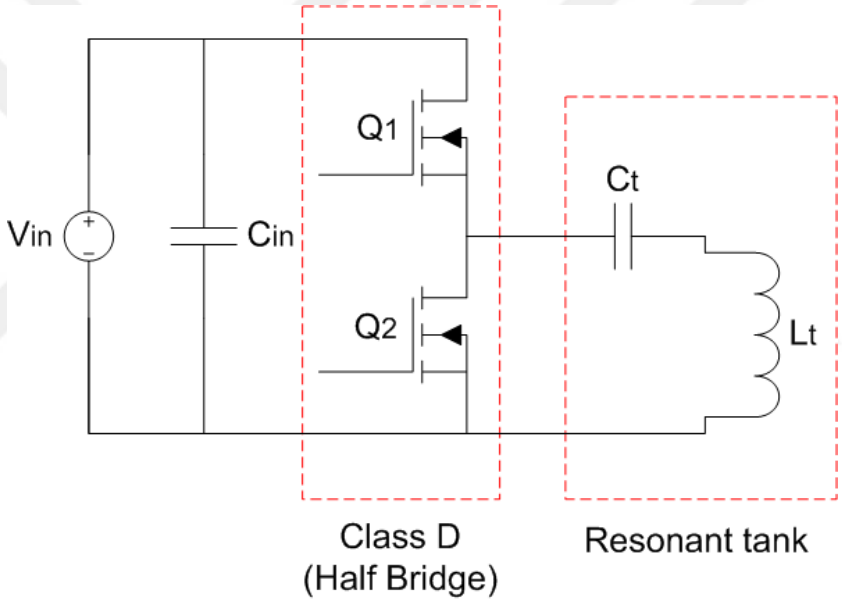

Figure 2.13: Class D (Half Bridge) driver circuit

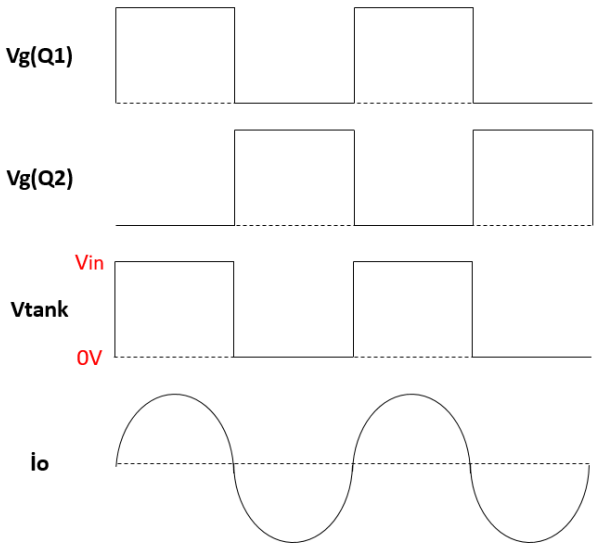

Figure 2.14: Waveforms of Class D (Half Bridge)

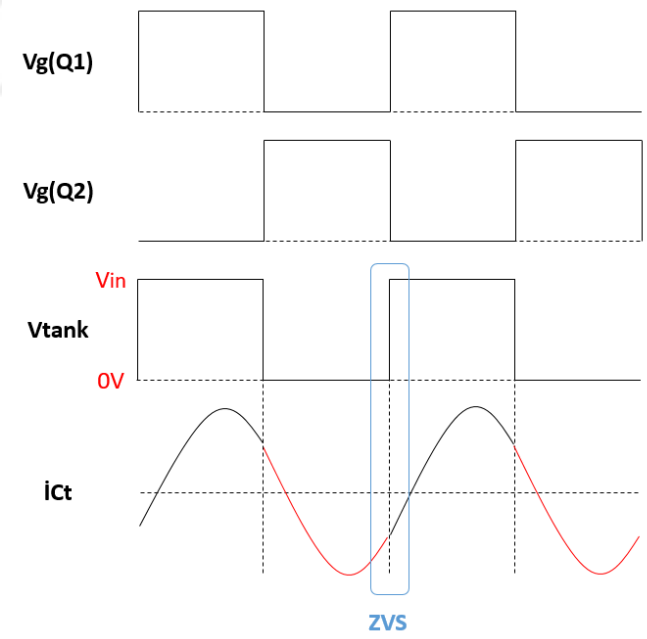

Figure 2.15: Waveforms of Class D (Half Bridge) with LLC compensation

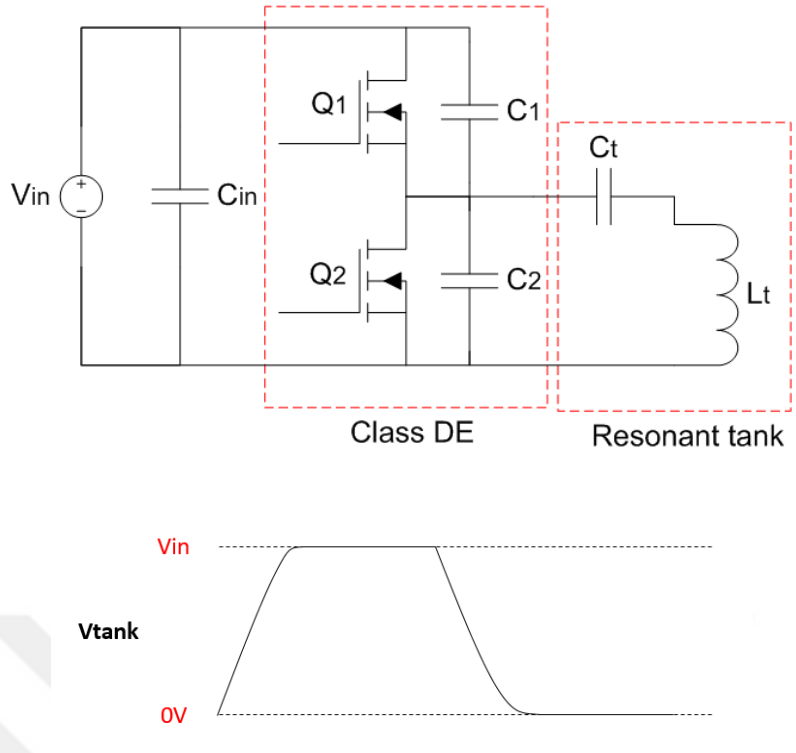

Figure 2.16: Class DE driver circuit

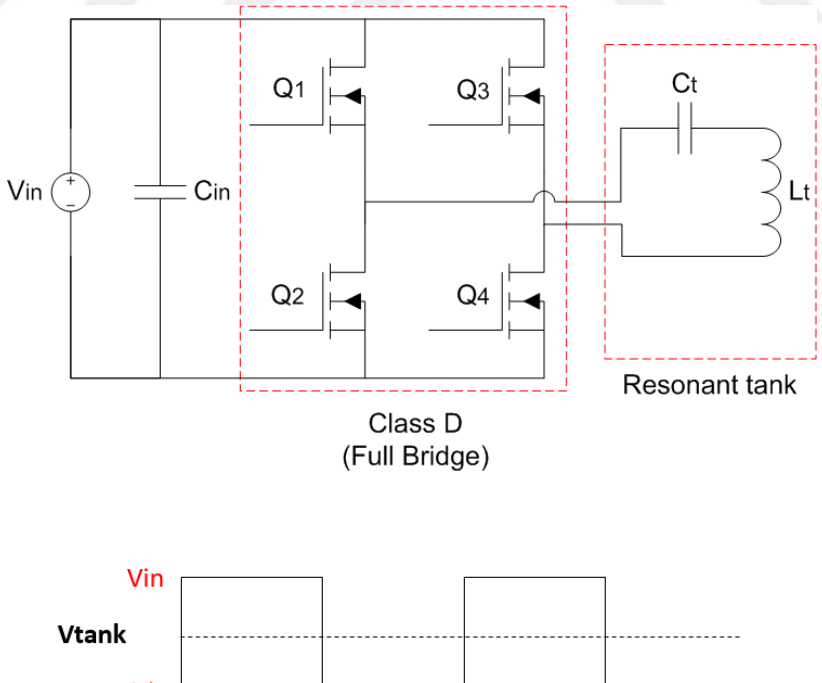

Figure 2.17: Class D (Full Bridge) driver circuit

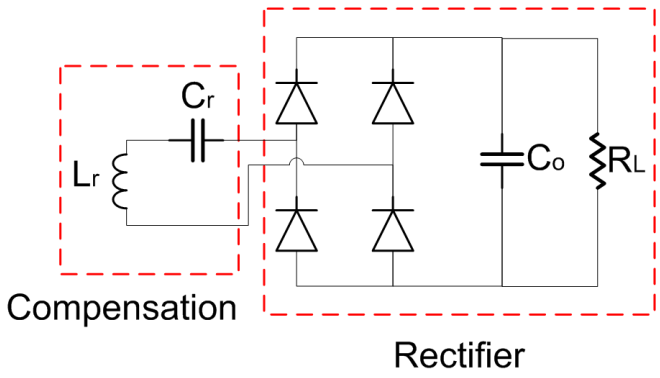

a)

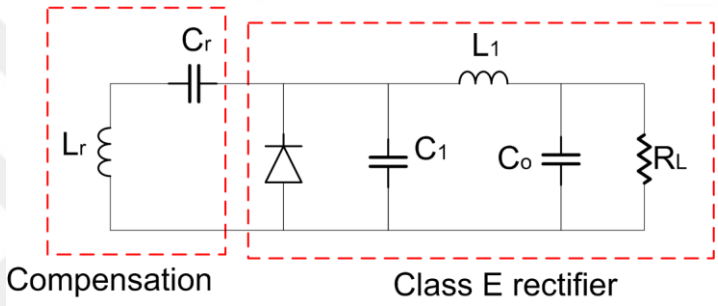

b)

Figure 2.18: Rectifier types in receiver

2.4 Coil Design for Wireless Power Transfer

Coil design is the most critical step in wireless power transfer application. It determines the performance of the system. Geometry, area, turns ratio, inductance and losses of coil are the parameters that must be considered. Homogeneous distribution of magnetic fields on coil is important for misalignment in inductive method. According to the (1), as the distance from wire, which carries current, increases; magnetic field density could be low. Large coils may have low magnetic field density in the center of it.

Spiral coil inductances are calculated from formula which is given by,

$$L = N^2 . 0{,}35 . d_{out} . 10^{\frac{d_{in}}{d_{out}}} \tag{28}$$

$$d_{out} = d_{in} + 2W \tag{29}$$

$$W = Nw + (N - 1)s \tag{30}$$

d_{in} is the inner diameter of the coil in meters, d_{out} is the outer diameter of the coil in meters, N is the turns ratio, W is the width of the coil in meters, w is the wire diameter in meters and s is the distance between windings in meters [11]. In Figure 2.19, r is shown as inner radius. According to (28) and (29), increasing the turns ratio and inner diameter are the most effective ways to get larger inductances.

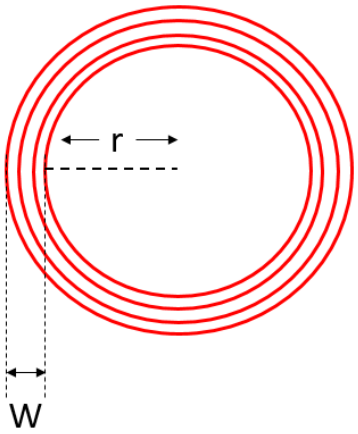

Figure 2.19: Parameters of coil

$$V = N.A.j\omega.B \tag{31}$$

The induced voltage in the receiver coil is related to turns ratio and area of receiver coil, frequency and magnetic field density generated by transmitter [11]. These factors affect the maximum power transferred to the load. Receiver coils with larger area have much more power [11].

$$P_{max} = Q\frac{{V_r}^2}{4\omega L_r} \tag{32}$$

According to the (9), high frequency operation has higher quality factor when they have the same inductance values. 6,78MHz of A4WP has the frequency advantage in compare to 200kHz of Qi. Inductance value could be increased in order to get high Q value. But, both high frequency and high inductance values may cause higher losses which decreases Q factor.

Despite the benefit of high frequency on Q, it causes increasing of switching losses on switching devices. Some losses on coils are also caused by high frequency operation. Radiation loss affects the system above 10MHz. It could be neglected for near field applications. Conduction losses occur based on skin effect and proximity effect.

While the direct current is flowing through the wire, DC loss occurs due to the resistance of it [24]. Skin effect is occured because of the alternating current. As the frequency increases, flowing current through the wire is dissipated only near the surface instead of whole cross-sectional area of wire. The reason of flowing on surface is the magnetic fields at high frequency. Surface of the wire shows high resistance in compare

to the whole area of wire. In high frequency operations, multiple-wire is used to increase the surface area (litz wire). ρ is the resistivity of the conductor, δ is the skin depth which is the distance from outer diameter to conducting place, μ is the permeability of the conductor [25].

$$R = \rho \frac{l}{A} \tag{33}$$

$$\delta = \sqrt{\frac{2\rho}{\omega\mu}} \tag{34}$$

The proximity effect is caused by other conductors' magnetic fields that are near to it. This is affected from winding structure and frequency of current. Insulation of wires may decrease the loss.

CHAPTER III

DESIGN OF COMBO WIRELESS CHARGING SYSTEM WITH CONTINUOUS RANGE COVERAGE FOR WEARABLE DEVICES

In the proposed wireless charging system, two standards are used with A4WP as a high frequency system and Qi as a low frequency system. Two coils are designed as transmitter coils and one coil is designed as a receiver coil. The circuit is created corresponding to drive each coil separately.

3.1 Combo Driver Circuit Structure

The schematic of proposed circuit is shown in Figure 3.1. The system involves two drivers working at order of magnitude different frequencies driving two independent co-centric coils in series resonance. Overall combo system is supplied from the same single standard 5V usb adapter. Firstly, two different driver circuits are implemented with the possibility to optimize each of the systems independently as well. This is done as such to be able to compare performances of all three cases: Qi only, A4WP only and combo system. Each one is optimized independently for maximum power transfer to the same exact receiver load. 100Ω is used as a load at receiver side to simulate wearable device (R_o). A4WP subsystem is optimized at 6,78MHz and Qi is optimized at the higher end of its standard at 230kHz. The receiver is designed as a wideband receiver coil to be able to receive the both frequency signals.

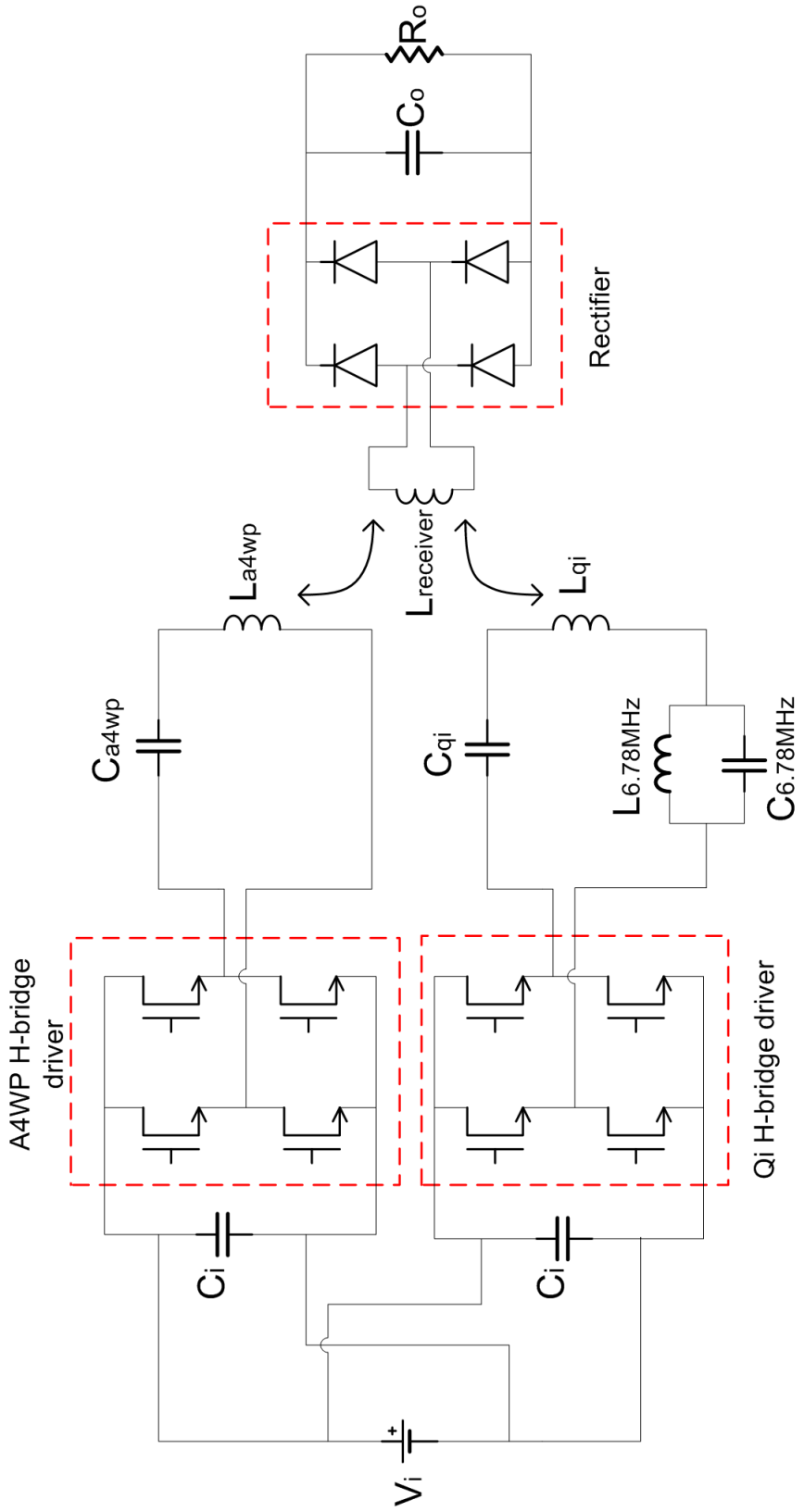

Figure 3.1: A schematic of combo wireless power transfer system

DRV8837 low voltage H-bridge driver chip is chosen as a driver of 230kHz circuit. V_m and V_{cc} pins are supplied by 5V from adapter and *IN1-IN2* pins are the input of the frequency signal. This chip is used because of its small size and low-cost advantages. It doesn't require external MOSFET usage.

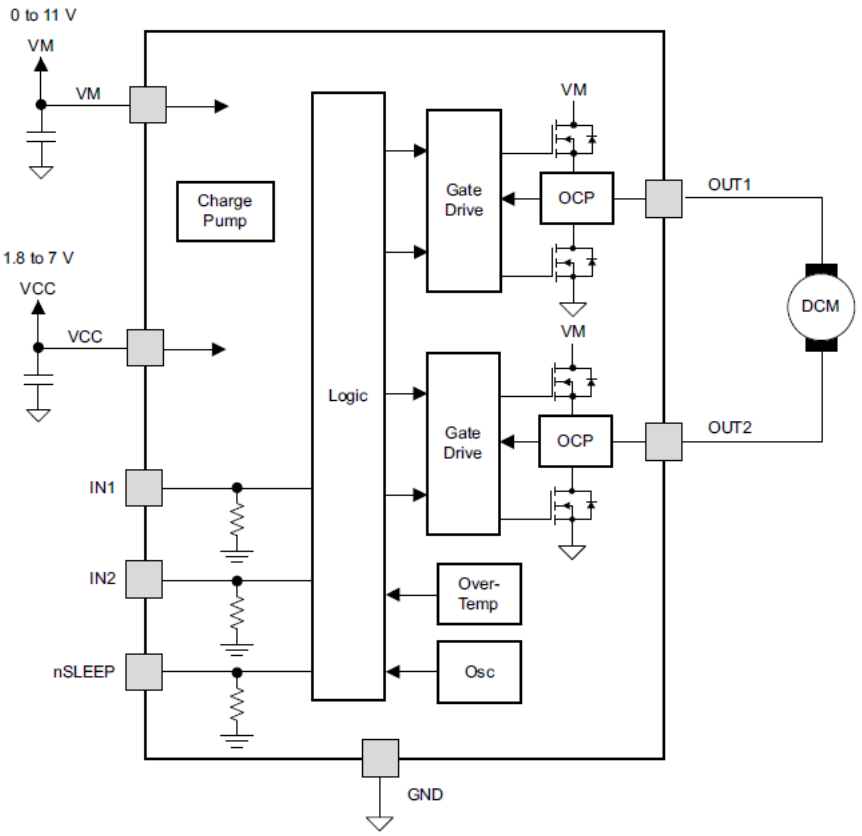

Figure 3.2: DRV8837 Functional block diagram [26].

For the 6,78MHz operation, DRV8837 couldn't be used due to its high rise and fall times. Thus, ISL89412 high speed, dual channel power MOSFET driver chip was chosen. It could give complementary outputs, so it is able to use as a driver without any switching devices. It has low rise and fall times which causes high frequency operation. However, its pull-up and pull-down resistances are high to decrease efficiency.

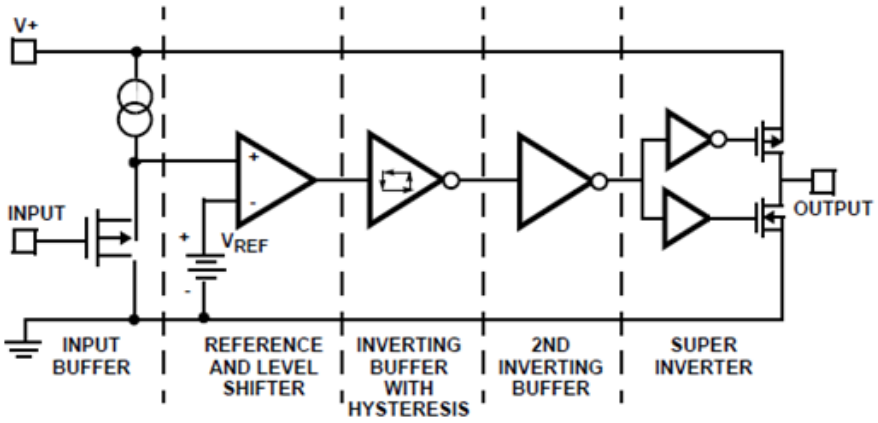

Figure 3.3: ISL89412 Functional block diagram [27].

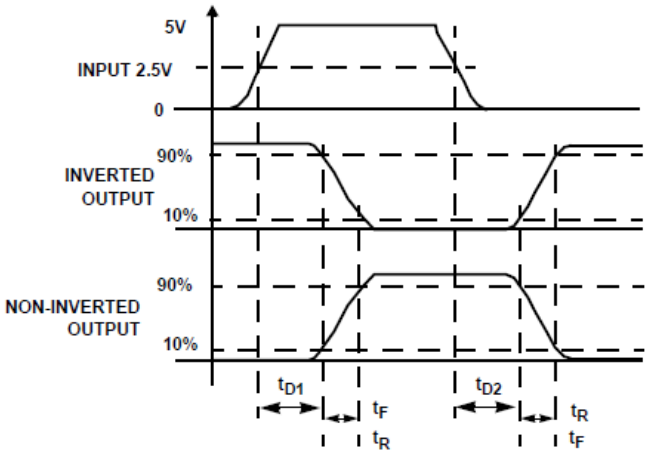

Figure 3.4: Timing of outputs [27].

In the receiver side, rectifier chip must be used which is able to work at both high and low frequency. Thus, BAS3007A chip was chosen which is very suitable to it. It is a low V_f schottky diode array chip which its each low diode capacitance is about 9pF. It has 0,3V forward voltage drop which causes decreasing efficiency on the receiver side.

3.2 Design of Coils

During the design of Qi transmitter coil, A4WP transmitter coil and receiver coil; a lot of coils are tried to optimize them according to their inductance value, size, internal resistance and turns ratios. The proposed coil placement would be in Figure 3.5.

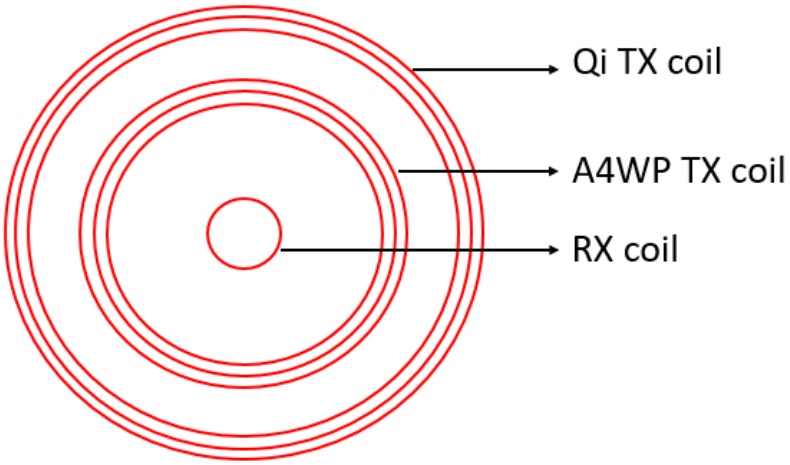

Figure 3.5: Placement of concentric coils

1) 2) 3)

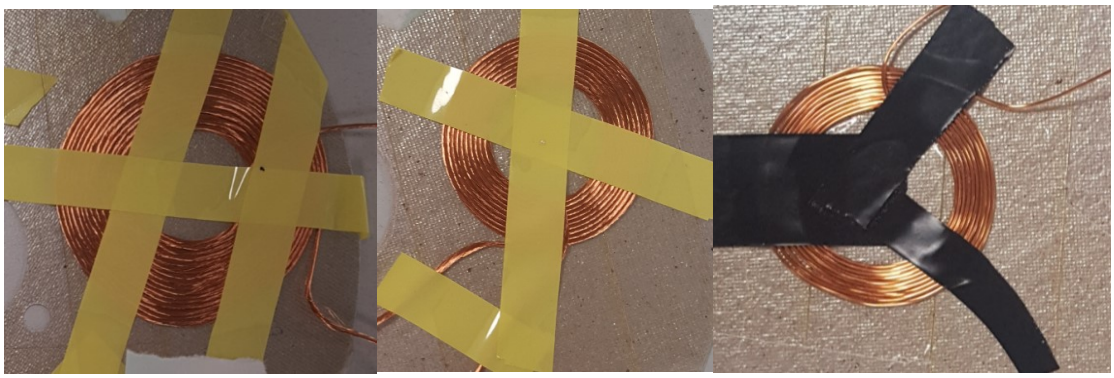

4) 5) 6)

Figure 3.6: A4WP transmitter coil trials

1. A4WP transmitter coil; 10Ts, 0,07mmx252N LITZ wire, diameter: 57mm, L=3,3µH
2. A4WP transmitter coil; 20Ts, 0,1mmx7N LITZ wire, diameter: 50mm, L=25µH
3. A4WP transmitter coil; 16Ts, 0,6mm UEW wire, diameter: 48mm, L=12µH
4. A4WP transmitter coil; 16Ts, 0,1mmx50N LITZ wire, diameter: 58mm, L=12µH
5. A4WP transmitter coil; 10Ts, 0,1mmx50N LITZ wire, diameter: 45mm, L=4,7µH
6. A4WP transmitter coil; 10Ts, 0,6mm UEW wire, diameter: 38mm, L=4,7µH

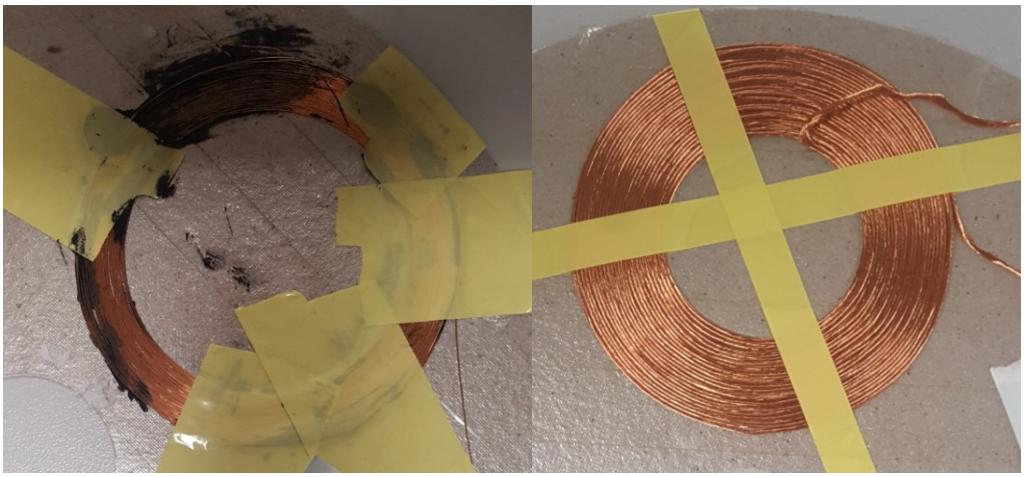

1) 2)

3)

Figure 3.7: Qi transmitter coil trials

1. Qi transmitter coil; 35Ts, 0,29mm UEW wire, diameter: 81mm, L=140µH
2. Qi transmitter coil; 25Ts, 0,1mmx50N LITZ wire, diameter: 100mm, L=100µH
3. Qi transmitter coil; 20Ts, 0,6mm UEW wire, diameter: 80mm, L=40µH

Sixth coil for A4WP and third coil for Qi were chosen to use. These coils are wrapped with UEW wires. Actually, LITZ wires must be used in high frequency systems, but LITZ wires causes drastically increase in size. In this application, coils are chosen with UEW wires when considered real product. Measured values and calculated values of inductances are close to each other. Measured values of inductances: L_{A4WP}=4,7µH; L_{qi}=40µH.

Calculated values in accordance with the formulas (28), (29) and (30):

For A4WP coil;

$$d_{in} = 24mm = 0{,}024m \tag{35}$$

$$d_{out} = 38mm = 0{,}038m \tag{36}$$

$$N = 10Ts \tag{37}$$

$$L = N^2.0{,}35.d_{out}.10^{\frac{d_{in}}{d_{out}}} = 5{,}69\mu H \tag{38}$$

For Qi coil;

$$d_{in} = 52mm = 0{,}052m \tag{39}$$

$$d_{out} = 80mm = 0{,}080m \tag{40}$$

$$N = 20Ts \tag{41}$$

$$L = N^2.0{,}35.d_{out}.10^{\frac{d_{in}}{d_{out}}} = 50\mu H \tag{42}$$

In order to improve the transfer efficiency, a ferrite sheet placed underneath the transmitter coils. After insertion of the ferrite layers, inductance values are increased as

7,65µH for A4WP coil and 68µH for Qi coil. These new inductance values were considered while tuning the driver circuit for resonance. On the other hand, the small receiver coil has 30Ts with total outer diameter of 15mm and wiring width of 1mm. The single wire width of the coil is very thin and the coil has multilayer structure winding to get large inner diameter. By using wire whose diameter is 0,15mm, small form factor receiver could be obtained. Thanks to large turn ratio, total inductance value was 19,5µH. Although the resultant series RX coil impedance was significant, it is not the limiting factor since the total power to be transferred was rather limited by the coil size.

Figure 3.8: Receiver coil

In accordance with the inductance values with ferrite sheet, capacitance values are calculated to resonance. 230kHz and 6,78MHz are considered as working frequencies. Capacitance is calculated by the formula (43) which is derived from formula (16). C_{A4WP} is calculated as 72pF, but 76pF capacitor is used in the system because of its tolerances and parasitic effects at high frequency.

$$C = \frac{1}{4\pi^2 {f_{res}}^2 L} \tag{43}$$

$$C_{qi} = 7nF \tag{44}$$

$$C_{A4WP} = 72pF \quad (45)$$

Mutual inductances of three coils with respect to each two coils are measured after coils were implemented. Mutual inductance value shows how they affect each other. By using mutual inductance value, coupling coefficients are calculated. The coupling coefficient between Qi coil and receiver coil is the least because of their large size difference.

$$M_{A4WP-Qi} = 6{,}6\mu H \quad (46)$$

$$k_{A4WP-Qi} = 0{,}29 \quad (47)$$

$$M_{A4WP-receiver} = 3{,}75\mu H \quad (48)$$

$$k_{A4WP-receiver} = 0{,}31 \quad (49)$$

$$M_{Qi-receiver} = 3\mu H \quad (50)$$

$$k_{Qi-receiver} = 0{,}08 \quad (51)$$

3.3 Optimization of Parallel LC Filter

There was a main issue to be resolved in this particular combo scheme: the loss associated due to mutual loading of each coil since they are placed one inside the other. That was the loading on the Qi system due to high frequency A4WP system was left quite limited by choosing the 6,78MHz coil inductance practically highest possible and hence the series resonance capacitor minimal. In addition to reducing the loading effect on the Qi transmitter, this would help the self-quality factor of the original high frequency mode. In order to prevent the reverse leak of power from the 6,78MHz coil back into the 230-

KHz Qi transmitter as a loss, the proposed system implements a blocking parallel resonance through $L_{6,78MHz}$ and $C_{6,78MHz}$. In this case the parallel resonance blocking inductance was chosen as minimum as possible with respect to the coil inductance of the Qi system to minimize the loss due to impedance division.

After Qi transmitter and A4WP transmitter are optimized individually, the output stages are combined together as driving each at resonance and optimizing the blocking filter. This filter is needed to prevent power loss due to the leakage inductance between transmitter coils. The way of blocking the 6,78MHz signal wave on the 200kHz circuit is to add a low-loss parallel resonance LC filter. When parallel LC combination resonates at 6,78MHz, it theoretically poses high impedance to any coupling at 6,78MHz. In fact, internal resistances of components decrease the quality factor of the filter and the impedance of it does not come about to be very high. Better filter components were needed to reach a higher Q factor value. The higher the Q factor, the less damping there is and the rejection becomes more effective without undesired losses caused by this enhancement filter itself. According to the equation (9), higher inductance ensures better filtering due to high Q. On the other hand, the inductance value of the non-radiative filter must be very low to prevent power loss on Qi circuit. Graph of the Q factor values with effective coil impedance is shown in Figure 3.9.

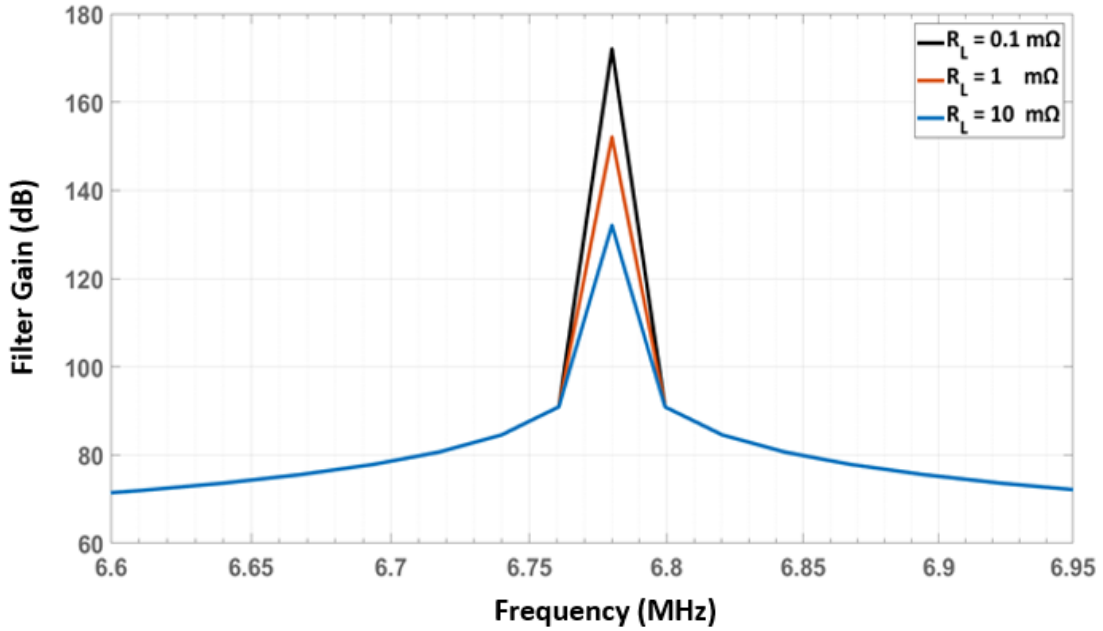

Figure 3.9: The bode diagram of *Q* factor of parallel LC filter by varying internal resistance of the inductor

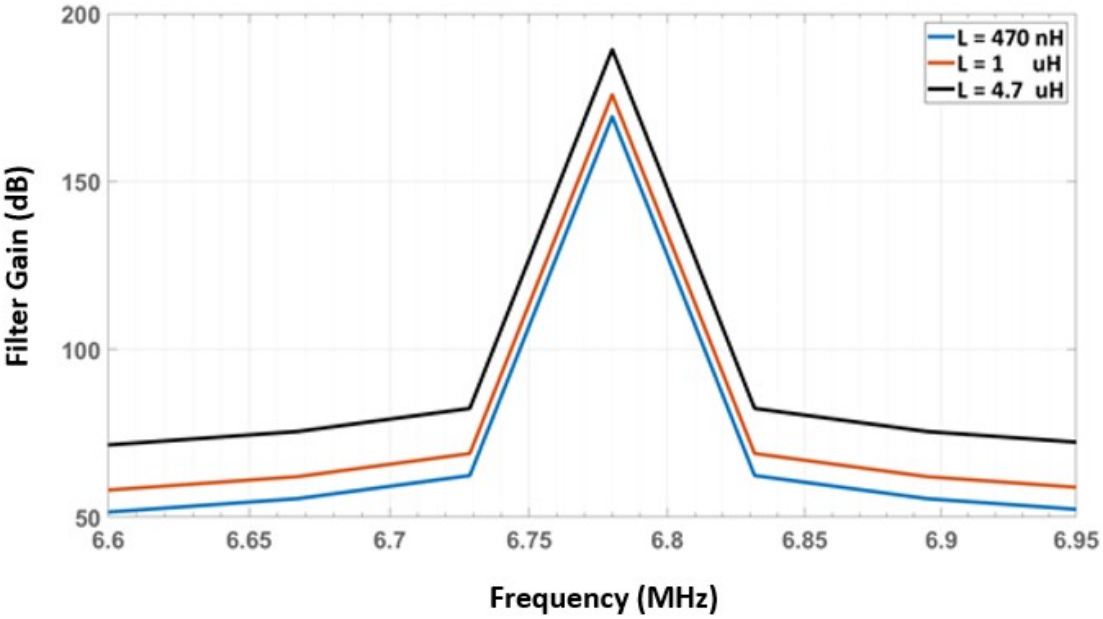

Figure 3.10: The bode diagram of *Q* factor of parallel LC filter by varying inductance value and capacitance value according to the resonance condition at 6,78MHz

The filter was tuned manually for once only to fit it best around the target center frequency to minimize the loss of A4WP transmitter leakage into Qi network. After the parallel LC filter components were tuned, Qi transmitter has to be compensated for resonance again because of change in the impedance of the filter. The component values and other parameters after the final optimization in the circuit are shown in Table 3.1. L_{a4wp} and L_{qi} coil inductance values assumed a ferrite shield as implemented in the test prototype system.

$$Z_L + Z_C + \frac{Z_{L_{6,78MHZ}} \times Z_{C_{6,78MHZ}}}{Z_{L_{6,78MHZ}} + Z_{C_{6,78MHZ}}} = 0 \tag{52}$$

$$Z_L = j98{,}219 \tag{53}$$

$$Z_{L_{6,78MHZ}} = j6{,}7 \tag{54}$$

$$Z_{C_{6,78MHZ}} = -j7287{,}6 \tag{55}$$

$$Z_C = -j105, \qquad C = 6{,}6nF \tag{56}$$

Table 3.1: Parameters in the system

Symbol	Values of Parameters
C_{a4wp}	76pF
L_{a4wp}	7,6µH
C_{qi}	6.6nF
L_{qi}	68µH
$C_{6,78MHz}$	95pF
$L_{6,78MHz}$	4,7µH

3.4 Experimental Results

PCB layout is designed and components are mounted to the PCB. The circuit is supplied by 5V usb adapter. The proposed combo system with 6,78MHz parallel resonance blocking filter has been implemented and characterized in measurements. Figure 3.11 shows the picture of this experimental prototype of the proposed combo system on a ferrite shield.

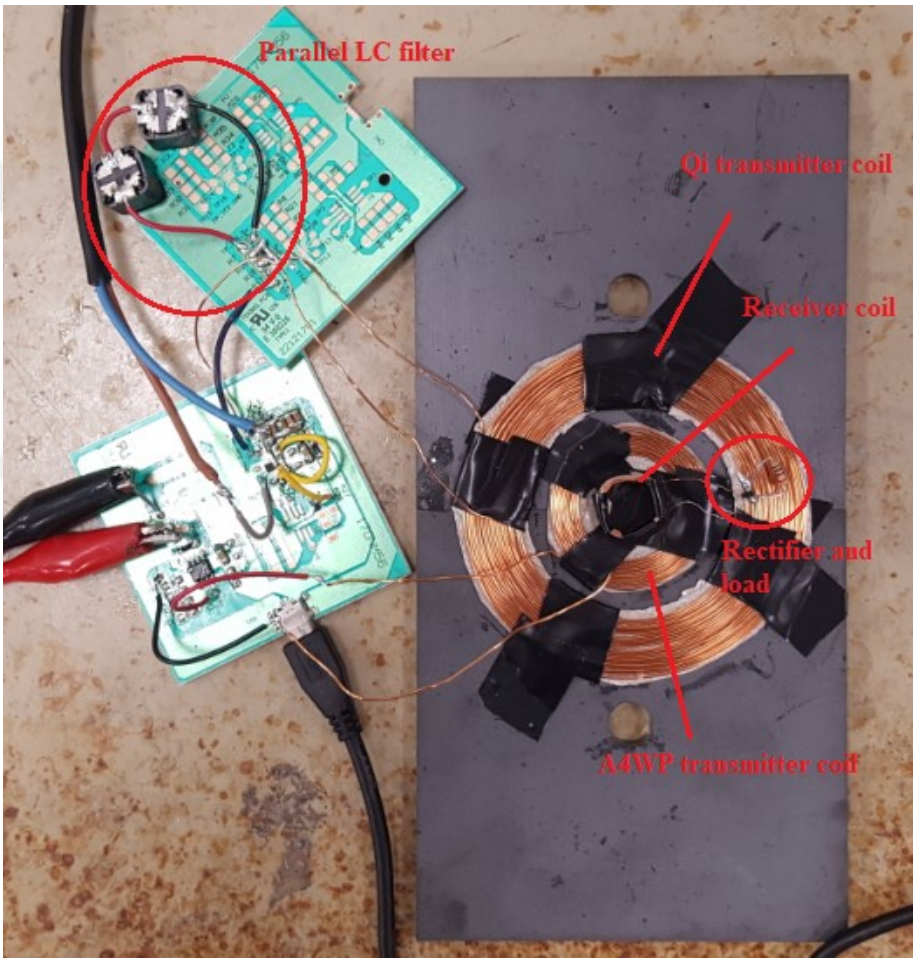

Figure 3.11: Experimental prototype of the proposed combo system

After all optimizations, the delivered power to the load according to the generated magnetic fields by transmitter coils along the X-axis, is simulated with MATLAB which is shown in Figure 3.12. Biot-Savart formula is used to calculate the distribution of

magnetic fields at any point above the circular coil [28]. Then, induced voltage on the receiver coil by using formula (31) and the power on the load could be calculated, respectively. The simulation is performed for three cases: Qi only, A4WP only and combo system. Simulation results show that the range of the delivered power to the load increases with the combo system. The transferred power level also increases in the combo system. In the simulation, the system is accepted as an ideal considering the infinite impedance of the LC filter for blocking 6,78MHz. Thus, the loss between high frequency and low frequency couldn't occur. In fact, power levels would be lower than simulation results due to losses on the coil and in the circuit. The loss on the A4WP system would be the drastically higher because of its very high operating frequency.

$$B_Z = \frac{\mu_0 NI}{2\pi\sqrt{(\rho+R)^2+z^2}} \times \left[K + \frac{E(R^2-\rho^2-z^2)}{(\rho-R)^2+z^2}\right] \tag{57}$$

$$K = \int_0^{\pi/2} \frac{d\psi}{\sqrt{1-k^2\,sin^2\,\psi}} \tag{58}$$

$$E = \int_0^{\pi/2} \sqrt{1-k^2\,sin^2\,\psi}\,d\psi \tag{59}$$

$$k = \sqrt{\frac{4R\rho}{\rho^2+z^2+R^2+2R\rho}} \tag{60}$$

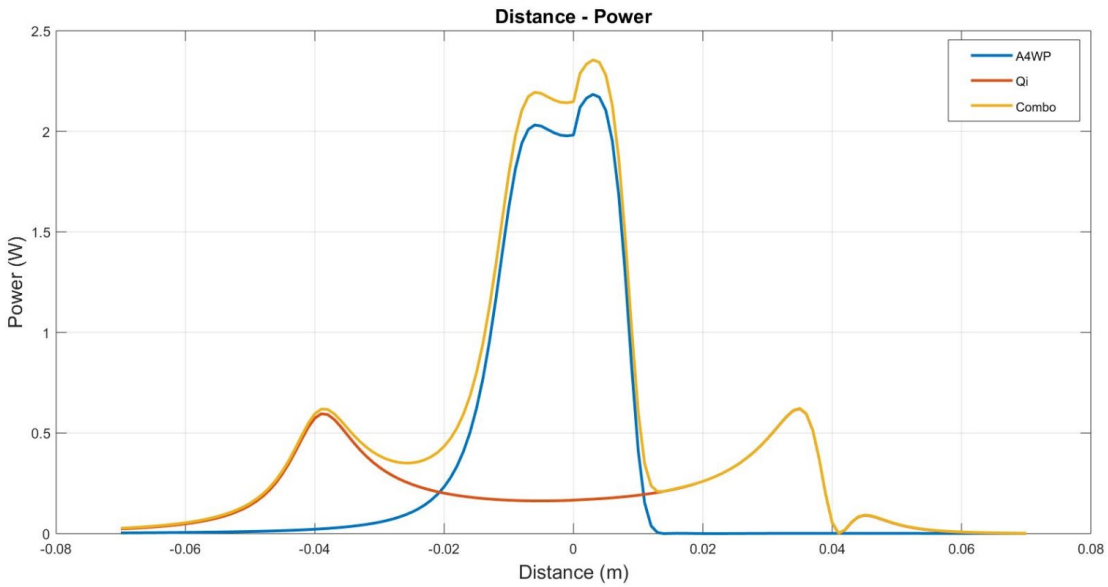

Figure 3.12: The simulation of the total transferred power with respect to the position of receiver coil for all 3 types transmitters

In the experimental study, the receiver coil is moved from -70mm to +70mm over the transmitter coils along the X-axis coordinates and the total transferred power is measured at a constant load R_O of 100Ω. This measurement is repeated for all three systems; namely, combo system, A4WP only system and Qi only system to get the spacial power transfer map for each design. A waveform generator is used to tune each of the sub-systems separately to their best resonance point with the load, in order to reach an apple-to-apple best obtainable performance comparison. The resulting power graph chart is shown in Figure 3.13. It may be seen in the figure that the proposed combo system could achieve significantly higher power transfer than A4WP system alone and again more power than Qi system alone around the central regions of the charging pad. It effectively combined the best of the two sub-systems and provided stable RX power levels across the whole charging pad scan area.

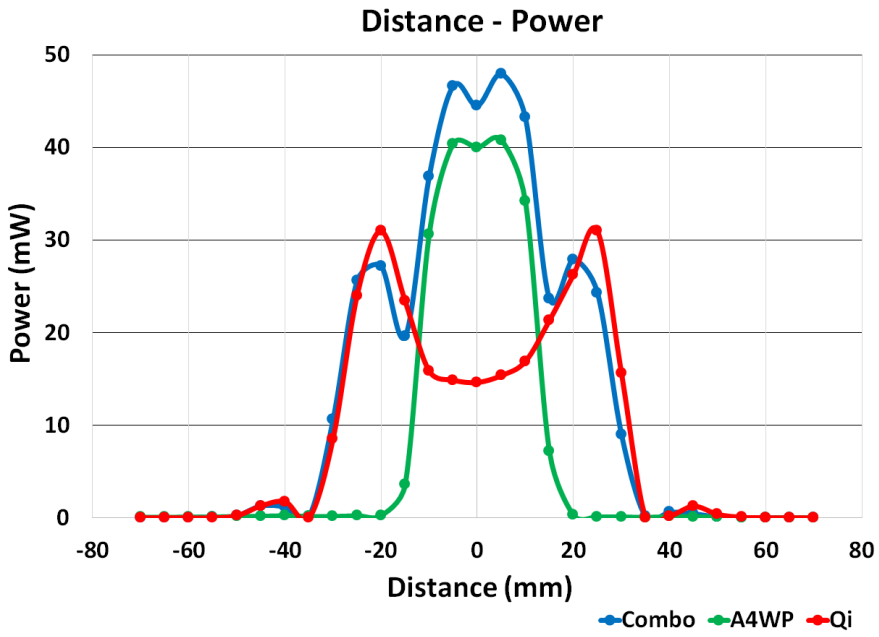

Figure 3.13: The total transferred power with respect to the position of receiver coil for all 3 types transmitters

Parallel LC resonant blocking filter effect is shown in Figure 3.14 and 3.15. The final rectified DC output voltage is measured as 1,907V on the 100Ω load and it corresponds to 36,36mW power transfer in the system without parallel LC filter when tuned for maximum possible level. Adding the filter and retuning the system increases the final rectified output voltage level to 2,113V increasing the total transferred power level to 44,64mW. Adding the filter reduced the power loss and increased total amount of transferred power level approximately by %23. Moreover, 6,78MHz noise reduction in I_{Lqi} was visible from difference in Figure 3.14 and 3.15 oscilloscope measurement plots.

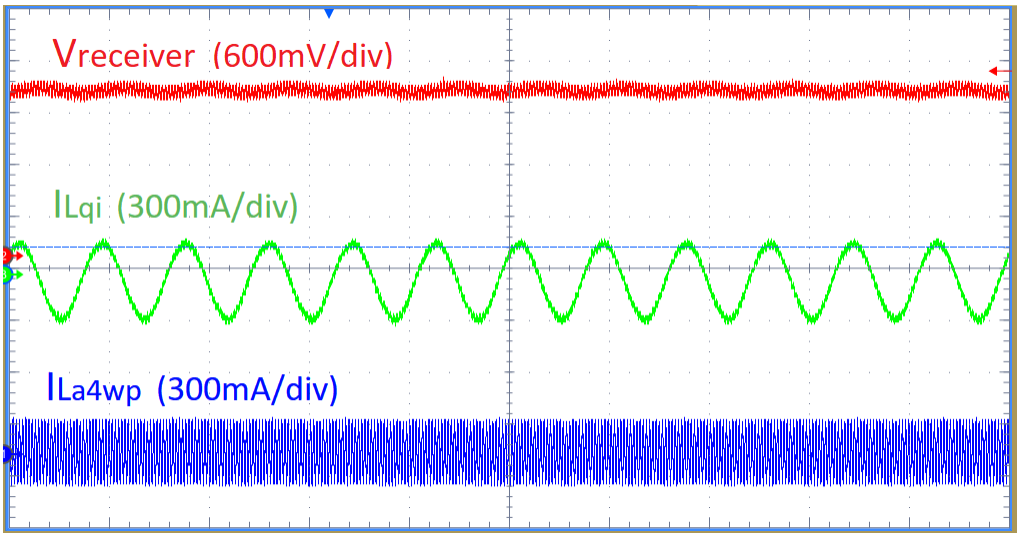

Figure 3.14: The output voltage and transmitter coil currents without parallel LC filter

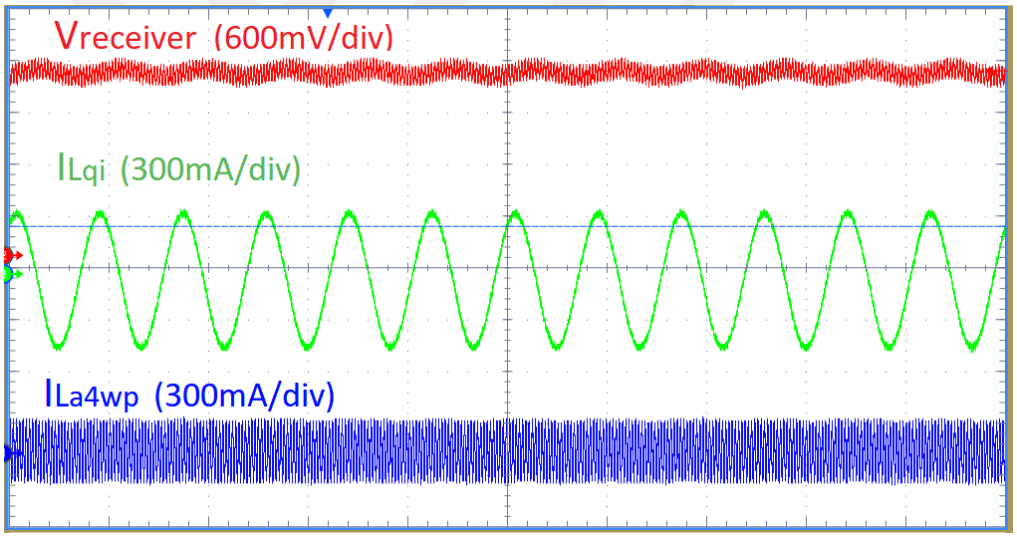

Figure 3.15: The output voltage and transmitter coil currents with the filter in place

Finally, in order to demonstrate the difficulty and hence the added value of more and spacially stable robust power distribution to small form factor wearable devices across the pad, the amount of power that could be transferred, is plotted in Figure 3.16 as a function of receiver coil size for the mentioned 30-turns schottky rectified receiver

design. It is quite clear that extracting useful amount of power, for coil radiuses below 10mm is a challenging task.

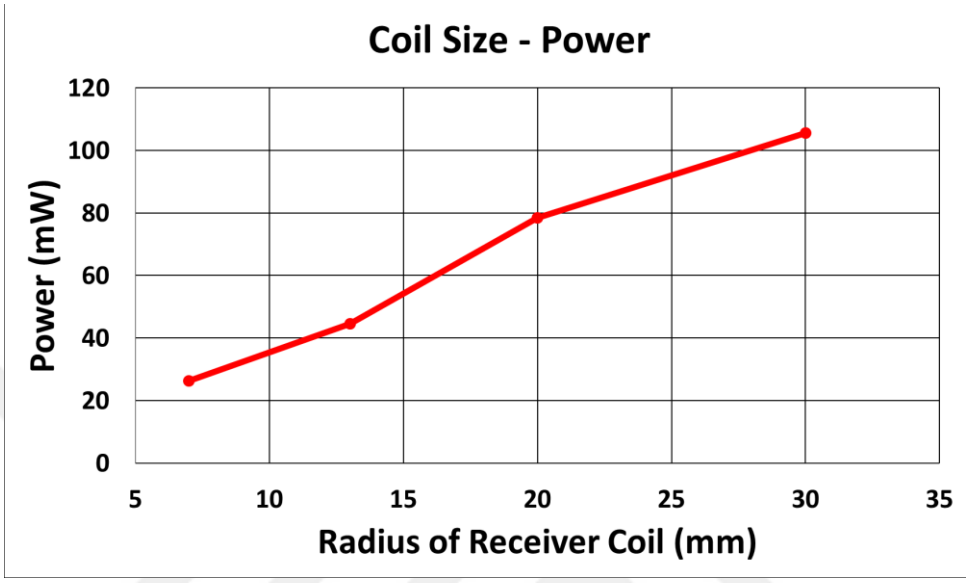

Figure 3.16: Measurement results for output power vs. 30-turn fixed coil radius

CHAPTER IV

CONCLUSION

This work has introduced a new combo wireless power transfer system for small size wearable device charging. The comparative study of the current competing charging standards were also involved in measurements to be able to draw fair conclusions regarding to the performance of the design. It has been shown that the combo design could provide not only more power in comparison to others but also it yielded uniform power with much wider spacial coverage without any snap or lock mechanism. Even more outstanding was that, the system was supplied from the same limited 5V standard USB wall charger power source in a similar pad area arrangement which also implied an apple-to-apple comparison. The work suggested that utilizing the both Qi and A4WP standards carefully with precision analog resonance loops could result in significant performance improvements.

APPENDIX A

MATLAB CODE FOR PLOTTING LOAD POWER

```
clc
close all
clear all

u=1.25*10^(-6);
Iqi=0.5;
Ia=0.04;
Nqi=20;
Na=10;
Rqi=0.04;
Ra=0.01;
p=[-0.07:0.001:0.07];
z=0.005;
kqi=sqrt(4*Rqi.*p./(p.*p+Rqi*Rqi+z.*z+2*Rqi.*p));
ka=sqrt(4*Ra.*p./(p.*p+Ra*Ra+z.*z+2*Ra.*p));

Kqi=ellipticF(pi/2,kqi);
Eqi=ellipticE(pi/2,kqi);
Ka=ellipticF(pi/2,ka);
Ea=ellipticE(pi/2,ka);

Bqi=(u.*Nqi.*Iqi.*(Kqi+((Rqi*Rqi-p.*p-z.*z).*Eqi)./((p-Rqi).*(p-
Rqi)+z.*z))).(2*pi.*sqrt((p+Rqi).*(p+Rqi)+z.*z));
```

```
Ba=(u.*Na.*Ia.*(Ka+((Ra*Ra-p.*p-z.*z).*Ea)./((p-Ra).*(p-
Ra)+z.*z))./(2*pi.*sqrt((p+Ra).*(p+Ra)+z.*z));


Ar=pi*0.014*0.014;

Nr=30;

Vqi=Nr.*Ar.*2.*pi.*230000.*abs(Bqi);

Va=Nr.*Ar.*2.*pi.*6780000.*abs(Ba);

Pqi=(Vqi.*Vqi)./100;

Pa=(Va.*Va)./100;

plot(p,Pa,p,Pqi,p,Pqi+Pa)
```

BIBLIOGRAPHY

[1] M. M. El Rayes, G. Nagib, W. G. A. Abdelaal, "A Review on Wireless Power Transfer," International Journal of Engineering Trends and Technology, vol. 40, pp. 272- 280, Oct 2016.

[2] A. K. Sah, "Design of Wireless Power Transfer System via Magnetic Resonant Coupling at 13.56MHz," in Proc. IOE Graduate Conf., vol. 1, pp. 202- 210, Nov 2013.

[3] WPC, https://www.wirelesspowerconsortium.com.

[4] M. Shidujaman, H. Samani, M. Arif, "Wireless Power Transmission Trends," 3rd International Conference on Informatics, Electronics & Vision 2014.

[5] C. Nataraj, S. Khan, F. F. Eniola and S. K. Selvaperumal, "Design of simple DC-to-DC wireless power transfer via inductive coupling," 3rd International Conference on Advances in Electrical, Electronics, Information, Communication and Bio-Informatics, Feb. 2017.

[6] R. Vinge, "Wireless energy transfer by resonant inductive coupling," Master's Thesis, Chalmers University of Technology, Göteborg, 2015.

[7] M. Kesler, "Highly resonant wireless power transfer: safe, efficient, and over distance," WiTricity Corporation, 2017.

[8] P. Belleau, "Wireless power for portable devices," Arrow Electronics, Jan. 2016.

[9] Wireless Power Consortium, "The Qi Wireless Power Transfer System Power Class 0 Specification," V1.2.3, Feb 2017.

[10] M. Galizzi, M. Caldara, V. Re and A. Vitali, "A novel qi-standard compliant full-bridge wireless power charger for low power devices," in Proc. IEEE WPT, pp. 44–47, 2013.

[11] E. Waffenschmidt, "Wireless power for mobile devices," in Proc. IEEE INTELEC, pp. 1-9, 2011.

[12] Würth Elektronik, "Wireless Energy Transmission Coils as Key Components," Application note, 2013.

[13] M. O. Abouzeid and A. Tekin, "Adaptive 6.78-MHz ISM band wireless charging for small form factor receivers," in Proc. IEEE ISCAS, pp. 1-4, 2017.

[14] Y.-J. Park, B. Jang, S.-M. Park, H.-C. Ryu, S. J. Oh, S.-Y. Kim, Y. Pu, S.-S. Yoo, K. C. Hwang, Y. Yang, M. Lee and K.-Y. Lee, "A triple-mode wireless power-receiving unit with 85.5% system efficiency for a4wp, wpc, and pma applications," IEEE Trans. Power Electronics, vol. 33, no. 4, pp. 3141-3156, Apr 2018.

[15] B. Johns, T. Antonacci and K. Siddabattula “Designing a qi-compliant receiver coil for wireless power systems, part1,” TI. 2012. [Online] Available: https://www.mouser.com/pdfDocs/TI-Designing-a-Qi-compliant-receiver-coil.pdf

[16] M. X. Chen and K. W. E. Cheng, “Design of flat magnetic core for inductively coupled coils in high efficiency wireless power transfer application,” in Proc. Intern. Conf. PESA-Smart Mobility, Power Transfer & Security, pp. 1-7, 2017.

[17] T. Campi and S. C. M. Feliziani, “Magnetic shielding of wireless power transfer systems,” in Proc. Intern. Symp. EMC, pp. 422-425, 2014.

[18] D. Ahn, S. Kim, S.-W. Kim, J. Moon and I. Cho, “Wireless power transmitter and receiver supporting 200-kHz and 6.78-MHz dual-band operation without magnetic field canceling,” IEEE Trans. Power Electronics, vol. 32, no. 9, pp. 7068-7082, Sep. 2017.

[19] C. Zhao and D. Costinett, “GaN based dual-mode wireless power transfer using multifrequency programmed pulse width modulation,” IEEE Trans. Ind. Electron., vol. 64, no. 11, pp. 9165-9176, Nov. 2017.

[20] P. S. Riehl, A. Satyamoorthy, H. Akram, Y.-C. Yen, J.-C. Yang, B. Juan, C.-M. Lee, F.-C. Lin, V. Muratov, W. Plumb and P. F. Tustin, “Wireless power systems for mobile devices supporting inductive and resonant operating modes,” IEEE Trans. Microwave Theory and Techniques., vol. 63, no. 3, pp. 780-790, Mar. 2015.

[21] M. Rooij and Y. Zhang, “A 10 W multi-mode capable wireless power amplifier for mobile devices,” in Proc. IEEE PCIM, pp. 1-8, 2016.

[22] Chris Burket, “Wireless charging opportunities and challenges for wearables: one size does not fit all,” IEEE Power Electronics Magazine, vol. 4, no. 4, pp. 53-57, Dec. 2017, 10.1109/MPEL.2017.2761658.

[23] Y. M. Roshan and E. J. Park, “Design approach for a wireless power transfer system for wristband wearable devices,” IET Power Electronics, vol. 10, no. 8, pp. 931-937, Jun. 2017.

[24] ANSYS, “Wireless power transfer for EV,” Regional Conferences, 2011.

[25] A. Abdolkhani, “Wireless power transfer – fundamentals and technologies,” Book, Jun. 2016.

[26] Texas Instruments, “DRV883x low-voltage H-bridge driver,” Datasheet, Feb. 2014.

[27] Renesas, “ISL89410, ISL89411, ISL89412 high speed, dual channel power mosfet drivers,” Datasheet, Oct. 2015.

[28] Z. Luo and X. Wei, “Mutual inductance analysis of planar coils with misalignment for wireless power transfer systems in electric vehicle, ” IEEE Vehicle Power and Propulsion Conference, pp. 1-6, Oct. 2016.

VITA

Üstün Sağlam was born in 1992 in İzmir. He received the B.S. degree in electrical and electronics engineering from Hacettepe University, Ankara, Turkey in 2015. Since 2016, he has been candidate of M.Sc. degree in electrical and electronics engineering at Ozyegin University.

Since 2015, he has been working at Vestel Electronics as a power electronics design engineer in Manisa, Turkey. His research interests include the design and the development of switched mode power supplies and wireless power transfer systems.